

## REPORT 1272

# A REEVALUATION OF DATA ON ATMOSPHERIC TURBULENCE AND AIRPLANE GUST LOADS FOR APPLICATION IN SPECTRAL CALCULATIONS <sup>1</sup>

By HARRY PRESS, MAY T. MEADOWS, and IVAN HADLOCK

### SUMMARY

*The available information on the spectrum of atmospheric turbulence is first briefly reviewed. On the basis of these results, methods are developed for the conversion of available gust statistics normally given in terms of counts of gusts or acceleration peaks into a form appropriate for use in spectral calculations. The fundamental quantity for this purpose appears to be the probability distribution of the root-mean-square gust velocity. Estimates of this distribution are derived from data for a number of load histories of transport operations; also, estimates of the variation of this distribution with altitude and weather condition are derived from available data and the method of applying these results to the calculation of airplane gust-response histories in operations is also outlined.*

### INTRODUCTION

During the last few years, advances have been made in the analysis of airplane behavior in rough air through the application of the theory of random processes and the techniques of generalized harmonic analysis (refs. 1 to 7). The application of these techniques is based upon the representation of atmospheric turbulence as a continuous random disturbance characterized by power-spectral-density functions and certain probability distributions. The power spectrum of the turbulence is then used along with the airplane response characteristics to determine the power spectra and other statistical characteristics of the airplane loads or motions in rough air. The application of this approach to the problem of calculating load and other histories for operational flight requires detailed information on the spectrum of turbulence in the atmosphere. The information required may be considered of two types: detailed information on the spectrum of turbulence and its variations, and information on the probability of encountering the various spectra.

A few measurements of the power spectrum of atmospheric turbulence have so far been made and are briefly reviewed in the report. These measurements indicate that, over most of the frequency range of interest, the spectra are inversely proportional to the square of the frequency and may be approximated by simple analytic expressions such as have been used in wind-tunnel studies of isotropic turbulence.

Also, the intensity of the turbulence as given by the root-mean-square gust velocity varied appreciably with the weather conditions. These results thus appear to provide some information on the power spectrum and its variations. They do not, however, provide any information of the second type required, that is, information on the probability of encountering the various spectra in actual operations. The purpose of this report is to provide information of this second type, that is, information on the probabilities of encountering the various conditions of turbulence.

The only source of information on the probability of encountering the various conditions of atmospheric turbulence appears to be the considerable amount of statistical data concerning atmospheric turbulence and airplane loads in rough air that has been collected by the National Advisory Committee for Aeronautics in the last 20 years. (See, for example, refs. 8 to 12.) These data have been obtained, in most cases, from airplane acceleration measurements in normal operations, although in some instances (ref. 10) the data were obtained in special flight investigations. These data are generally given in the form of the number of peak accelerations or effective (or "derived") gust velocities per second which exceed given values and in this form do not appear applicable to spectral methods of analysis.

Fortunately, in the theory of random processes, relations have been derived (ref. 13) between peak counts (such as have been made for normal acceleration) and the associated power spectra. These relations apply to the case of a stationary Gaussian random process, the stationarity of the process implying that its characteristics do not change with time and the term Gaussian designating a process characterized by a Gaussian probability distribution for the amplitude of the disturbance as well as for its time derivatives. The approximately Gaussian character of turbulent velocity fluctuations has been noted and, for the case of atmospheric turbulence, results reported, for example in reference 3, appear to support such an assumption. Inasmuch as the intensity of turbulence is known to vary widely with weather conditions, the overall gust and load experience in operations cannot be considered a stationary Gaussian process. If the operational gust history is

<sup>1</sup> Supersedes NACA Technical Notes 3382 by Harry Press, May T. Meadows, and Ivan Hadlock, 1955, and 3540 by Harry Press and May T. Meadows, 1955.

considered to be a nonstationary Gaussian process varying only in intensity or root-mean-square gust velocity, the problem of specifying the gust history is reduced to that of specifying the probability distribution of the root-mean-square gust velocity. For this case, it appears possible to extend the results of reference 13 for the stationary Gaussian process in order to derive a basis for estimating the distribution of root-mean-square gust velocity from counts of acceleration peaks.

On the basis of the foregoing considerations, techniques are developed in this report for the estimation of the probability distributions of the root-mean-square acceleration and root-mean-square gust velocity from data on peak gust accelerations. Two approaches are considered: first, that the root-mean-square gust velocity takes on only a few discrete values and, secondly and more realistically, that the root-mean-square values cover a continuous range of values. These techniques are then applied to available gust-load data obtained from a number of transport operations and the associated probability distributions of root-mean-square gust velocity are derived. Also, available data are used to estimate the variations in this distribution with altitude and weather condition. The method of application of these results to the calculation of gust-load and other airplane response histories in operations is outlined and some of the limitations of the present results are indicated.

**SYMBOLS**

- $\bar{A}_1 = \frac{\rho V S m}{2W} \sqrt{\frac{I(K,s)}{\pi}}$
- $a_n$  acceleration,  $g$  units
- $a_1, a_2, a_3$  scale parameters in distributions,  $f(\sigma_{a_n})$
- $b_1, b_2, b_3$  scale parameters in distributions,  $\hat{f}(\sigma_v)$
- $\bar{c}$  average chord, ft
- $f(\sigma_{a_n})$  probability density distribution of  $\sigma_{a_n}$
- $\hat{f}(\sigma_v)$  probability density distribution of  $\sigma_v$
- $\hat{F}(\sigma_v)$  cumulative probability distribution of  $\sigma_v$
- $g$  acceleration due to gravity, 32.2 ft/sec<sup>2</sup>
- $\left[ \frac{I(K,s)}{\pi} \right]^{1/2}$  airplane gust-response factor
- $K$  airplane mass parameter,  $\frac{4W}{g\pi\rho S\bar{c}}$
- $L$  scale of turbulence
- $\frac{L}{M(a_n)}$  average number of maximums per second exceeding given value of  $a_n$  in operations
- $m$  slope of lift curve per radian
- $N( )$  average number of maximums per second exceeding given value of specified argument for Gaussian disturbance

$$N_0 = \frac{1}{2\pi} \left[ \frac{\int_0^\infty \omega^2 \Phi(\omega) d\omega}{\int_0^\infty \Phi(\omega) d\omega} \right]^{1/2}$$

- $N_2 = N_0 e^{-2}$
- $P$  proportion of total flight time
- $S$  wing area, sq ft
- $s$  ratio of chord to turbulence scale,  $\bar{c}/L$
- $T$  specified time, sec
- $T(\omega)$  amplitude of airplane acceleration response to unit sinusoidal gusts of frequency  $\omega$
- $t$  time, sec
- $V$  true airspeed, fps
- $V_\infty$  wind speed, fps
- $W$  airplane weight, lb
- $y(t)$  random function of time
- $\bar{y}^2$  mean-square normal acceleration, ft/sec<sup>2</sup>
- $\rho$  air density, slugs/cu ft
- $\sigma$  root-mean-square deviation,  $(\overline{y^2(t)})^{1/2}$
- $\Phi(\omega)$  power-spectral-density function,  $\lim_{T \rightarrow \infty} \frac{1}{2\pi T} \left| \int_{-T}^T y(t) e^{-i\omega t} dt \right|^2$
- $\lambda$  gust wavelength, ft
- $\omega$  frequency, radians/sec
- $\Omega$  reduced frequency,  $2\pi/\lambda$ , radians/ft
- Subscript:
- $U$  gust velocity

**SPECTRAL CHARACTERISTICS OF ATMOSPHERIC TURBULENCE**

In the way of background for the present analysis, it will be helpful to review the available measurements of the power spectrum of atmospheric turbulence. Figure 1 contains a summary of most of the available airplane measurements of the power spectrum of atmospheric turbulence. The first of these measurements was made by Clementson at the Massachusetts Institute of Technology (ref. 4), and subsequent measurements were made by the National Advisory Committee for Aeronautics (refs. 5 and 7), Douglas Aircraft Company, Inc. (ref. 14), Massachusetts Institute of Technology (ref. 15), and Cornell Aeronautical Laboratory (refs. 16 and 17). The curves shown represent the various power spectra which were obtained under different weather conditions. The abscissa is the frequency argument  $\Omega$  which has the dimensions of radians per foot and is equal to  $2\pi$  divided by  $\lambda$ , the gust wavelength. (The data shown cover a range of gust wavelengths from about 10 feet to 5,000 feet.)

The spectra in all but one case are for the vertical or lateral component of the turbulence. In one case marked by the letter  $H$ , the spectrum is for the horizontal or longitudinal component of turbulence. Examination of these results indicates that the spectral shapes appear to be relatively consistent; in all cases, the power decreases rapidly with increasing frequency. In fact, in most cases, the spectra appear to be inversely proportional to the square of the frequency. This spectral shape of  $1/\Omega^2$  is in reasonable agreement with theoretical results obtained for the spectral shape at the

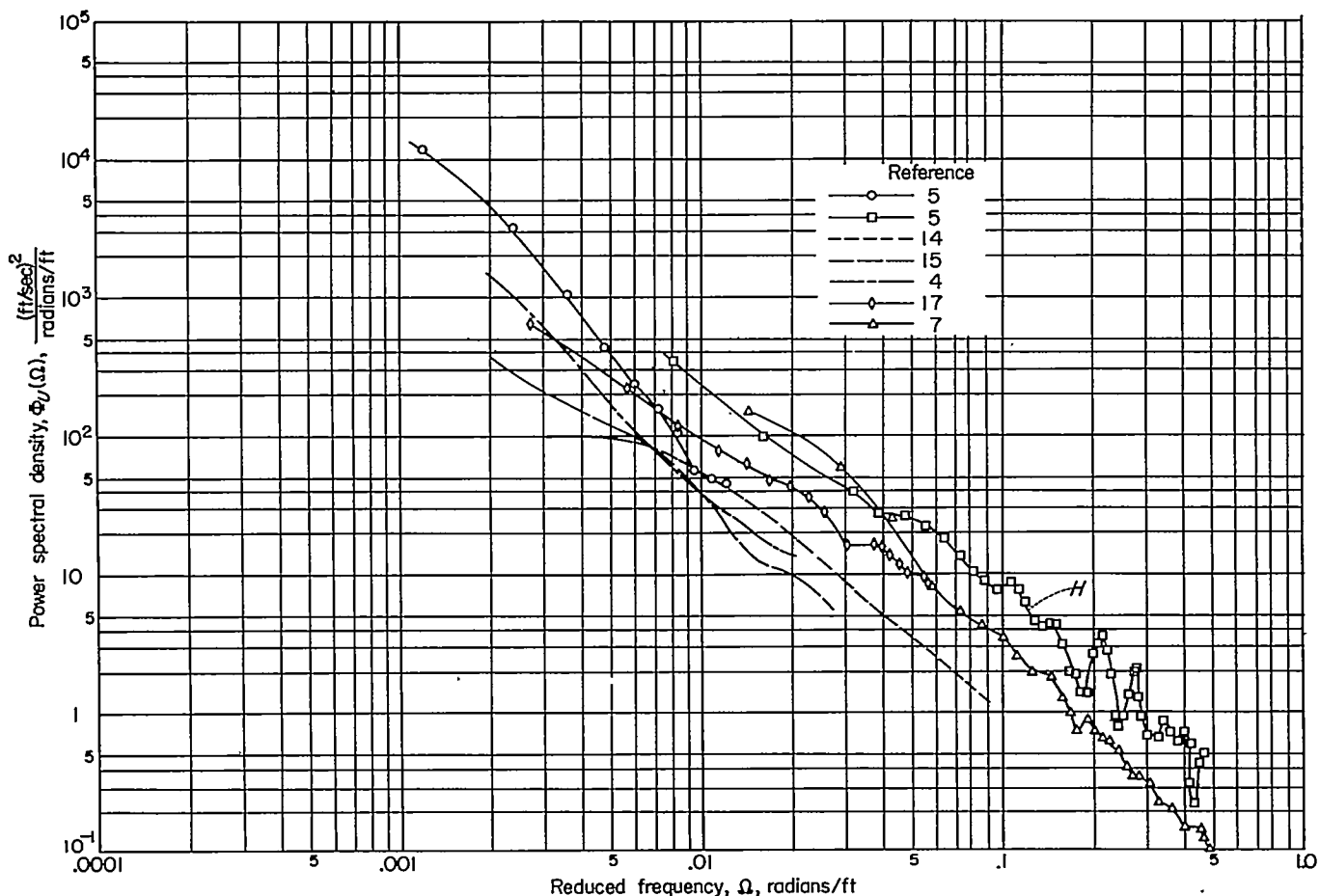


FIGURE 1.—Summary of airplane measurements of the power spectrum of atmospheric turbulence.

higher frequencies in the theory of isotropic turbulence. At the lower frequencies, the situation is not as clear, few measurements being available for frequencies  $\Omega < 0.002$ . Some additional measurements obtained at the Cornell Aeronautical Laboratory and at the NACA (ref. 18) do cover these lower frequencies and indicate a flattening of the spectrum at frequencies  $\Omega < 0.001$ .

In addition to these variations in spectral shape, the various measurements also differ in turbulence intensity. The individual root-mean-square values are estimated to vary from roughly 1.5 to perhaps 8 feet per second, which, as will be seen, represent the relatively light-to-moderate levels of atmospheric turbulence.

Another source of information on the spectral characteristics of atmospheric turbulence is the measurements at lower altitudes made from meteorological towers. A large number of such spectral measurements have now been obtained. A few representative measurements obtained at an elevation of about 300 feet and for various conditions of average wind speed  $V_w$  (ref. 19) are shown in figure 2. These measurements extend to lower frequencies (longer gust wavelengths) than do most of the available airplane measurements. At the higher frequencies, these results approximate the same form  $1/\Omega^2$  that is characteristic of the airplane

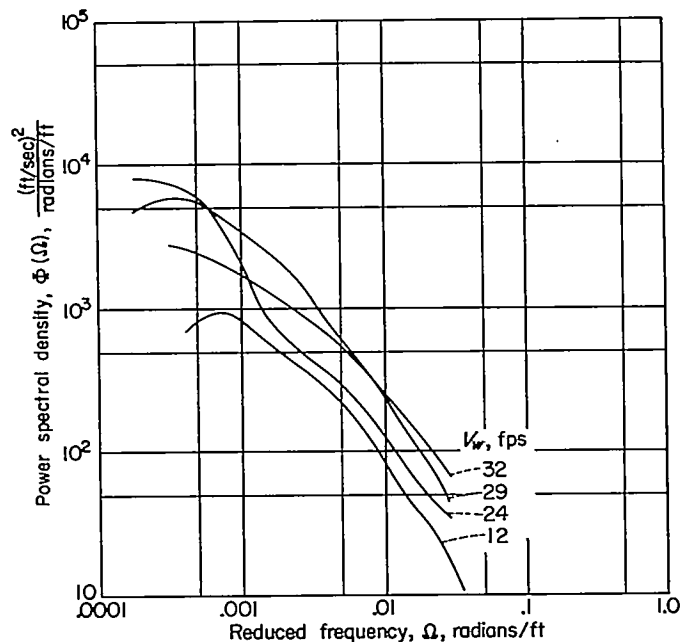


FIGURE 2.—Measurements of the power spectrum of atmospheric turbulence obtained at 300 feet from a meteorological tower (ref. 19).

measurements. In addition, at the lower frequencies, a definite tendency toward a flattening of the spectra can be noted. The variation in the spectrum intensity with wind speed  $V_w$  should also be noted.

Because of the general characteristics of these spectral measurements, it has been convenient in theoretical studies to use the following analytical expression for the turbulence spectrum

$$\Phi(\Omega) = \sigma_v^2 \frac{L}{\pi} \frac{1 + 3\Omega^2 L^2}{(1 + \Omega^2 L^2)^2} \quad (1)$$

where  $\Omega = 2\pi/\lambda$  and  $\lambda$  is the gust wavelength. This expression has been useful in wind-tunnel studies of turbulence and has the general characteristics of the measured spectra of atmospheric turbulence. The equation has two parameters: the mean-square gust velocity  $\sigma_v^2$  which describes the overall intensity, and the so-called scale of turbulence  $L$  which, in a sense, can be considered to be proportional to the average eddy size. Curves for this expression are shown in figure 3 for values of  $L$  of 200, 600, 1,000, and 2,000 feet. At higher frequencies, these curves all approach a shape of  $1/\Omega^2$  but differ in the frequency at which the flattening occurs. For increasing values of  $L$ , the curves flatten out at lower frequencies. Comparison of these curves with those of figures 1 and 2 and other measurements of the spectrum for atmospheric turbulence has indicated that the values of  $L$  for atmospheric turbulence are of the order of 1,000 feet. A value of 1,000 feet is used as a representative average value in the subsequent analysis.

For design purposes, the overall gust experience in operations is of concern. Presumably, the overall experience consists of various exposure times to each of the spectra shown in figures 1 and 2 as well as to other spectra associated with different weather conditions. It thus appears important to determine the proportion of flight time spent under these various conditions of turbulence. In the next section methods are developed for obtaining information on this problem from available gust statistics. These methods are then applied in a subsequent section.

### DERIVATION OF CONVERSION TECHNIQUES

#### BASIC METHOD

In the present analysis, use will be made of some concepts and results in the theory of random processes. The theory of random processes is a recently developed branch of probability theory and the aspects of the theory pertinent to the present applications are described in some detail in reference 13. In particular, the relations between peak counts and spectra for a stationary Gaussian random process which will be used in the present study are derived therein. Some general aspects of random-process theory are also covered in references 20 and 21.

In many recent studies of airplane behavior in rough air, atmospheric turbulence is generally considered a stationary Gaussian random process. The assumption that turbulence is a Gaussian random process appears warranted by the approximately Gaussian character of turbulent velocity fluctuations. The assumption of stationarity implies that

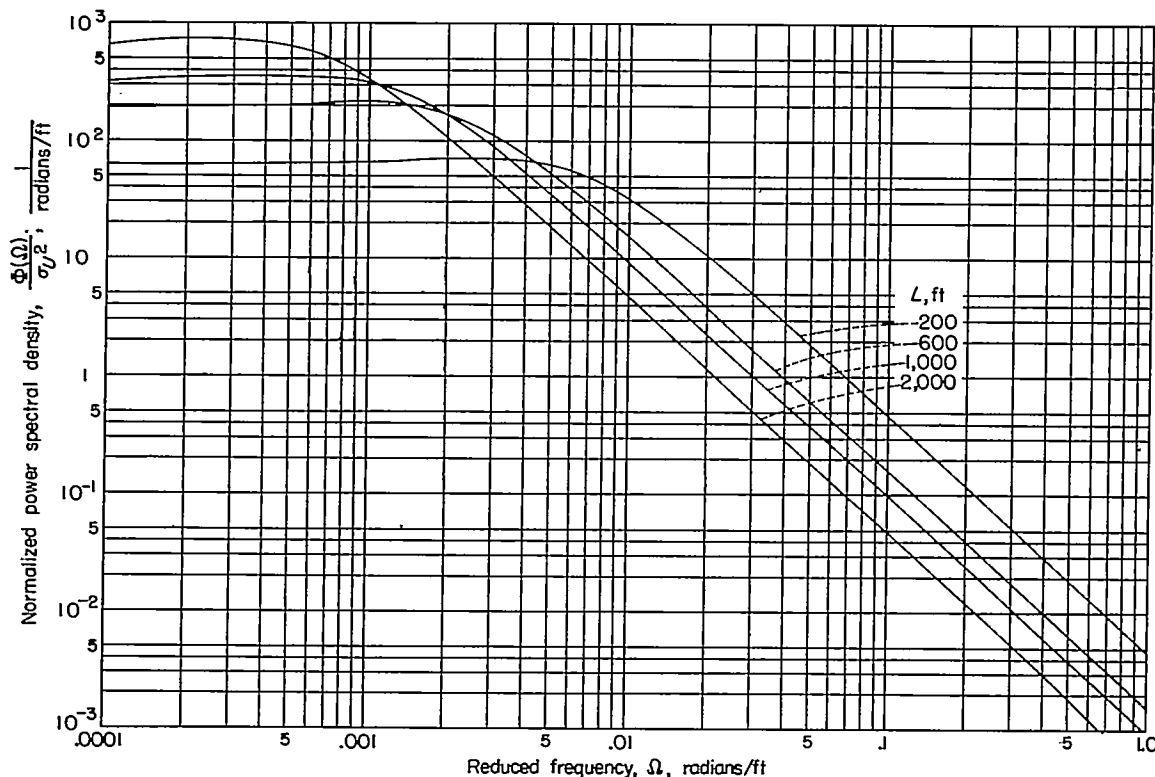


FIGURE 3.—Analytic representation of the spectrum of atmospheric turbulence.

$$\Phi(\Omega) = \sigma_v^2 \frac{L}{\pi} \frac{1 + 3\Omega^2 L^2}{(1 + \Omega^2 L^2)^2}$$

the statistical characteristics of the turbulence are invariant with space and time and also appears warranted for many purposes. For present purposes (in which the overall gust and load experiences of an airplane in operational flight are of concern), however, the process cannot be considered a simple stationary one, inasmuch as the turbulence characteristics of the atmosphere vary widely with weather conditions, particularly in regard to the intensity of the turbulence.

In order to account for the variations in atmospheric turbulence with weather condition, it will be assumed that turbulence is only locally Gaussian and stationary; that is, its statistical characteristics are Gaussian and invariant in a given restricted region and for a short time but vary, particularly in intensity, from time to time and place to place. This assumption implies that the region or time is small relative to the entire flight path or flight duration but large enough for statistical equilibrium to be achieved. The Gaussian character for the turbulent velocity fluctuations for a given weather condition will be used as a building block to construct the operational gust history, which must cover many weather conditions and, in the overall, is not a stationary Gaussian process. On this basis, the overall turbulence experienced by an airplane in given operations is taken to consist of the summation for appropriate exposure times to a series of elemental stationary Gaussian processes.

If the airplane response to turbulence is linear, as assumed in the present analysis, the response, such as the load history to each elemental turbulence process, is likewise a Gaussian process and the overall operational load history may in turn also be considered to consist of a summation of the loads for the various elemental Gaussian turbulence disturbances. This scheme serves to yield a reasonable approximation of the actual airplane load history and, further, has the particular advantage for present purposes of permitting the use of relations between peak counts and spectra derived for the stationary Gaussian case in reference 13.

The foregoing considerations form the basis for the present analysis. They will be applied in order to estimate the probability distribution of root-mean-square acceleration from operational data on peak accelerations. These estimates of the distribution of root-mean-square acceleration will then be used in order to obtain the associated probability distributions of root-mean-square gust velocity by taking into account the airplane dynamics.

**RELATIONS BETWEEN NUMBER OF PEAKS AND SPECTRA**

**Simple Gaussian case.**—The asymptotic relation between the average number of maximums per second exceeding a given value and the spectrum of a stationary Gaussian disturbance  $y(t)$  has been derived in reference 13 and is for large values of  $y$  given by (see appendix)

$$N(y) = \frac{1}{2\pi} \left[ \frac{\int_0^\infty \omega^2 \Phi(\omega) d\omega}{\int_0^\infty \Phi(\omega) d\omega} \right]^{1/2} e^{-y^2/2\sigma^2} \quad (2)$$

where

- $N(y)$  average number of maximums per second exceeding given values of  $y$
- $\omega$  frequency, radians/sec
- $\Phi(\omega)$  power-spectral-density function of random disturbance  $y(t)$

$$\sigma^2 = \int_0^\infty \Phi(\omega) d\omega$$

Equation (2) is the exact expression for the number of crossings per second with positive slope of given values of  $y$  but is an approximate expression for the number of maximums above a given value of  $y$ . For present purposes, however, equation (2) appears to be an adequate approximation of the number of peaks, as indicated in the appendix, and forms the basis for the present analysis.

Examination of equation (2) indicates that the number of peaks per second above given values depends upon  $\sigma^2$ , which is the area under the spectrum, and upon the second moment of the spectrum about the origin. If it is assumed that the spectral shape of turbulence is invariant with weather conditions (as suggested by available measurements) and varies only in intensity or root-mean-square gust velocity, the output spectrum  $\Phi_{a_n}(\omega)$  for acceleration  $a_n(t)$  for a given airplane under given operating conditions (fixed speed, weight, altitude, etc.) is likewise invariant in shape. Under these conditions, the coefficient of the exponential term in equation (2) is a fixed constant and equation (2) may be written as

$$N(a_n) = N_0 e^{-a_n^2/2\sigma^2} \quad (3)$$

where the constant  $N_0$  is given by

$$N_0 = \frac{1}{2\pi} \left[ \frac{\int_0^\infty \omega^2 \Phi_{a_n}(\omega) d\omega}{\int_0^\infty \Phi_{a_n}(\omega) d\omega} \right]^{1/2} \quad (4)$$

The constant  $N_0$  gives the expected number of times per second that  $a_n(t)$  crosses the value zero with a positive slope. Because of the invariance of the shape of  $\Phi_{a_n}(\omega)$ , the quantity  $N_0$  is independent of the turbulence intensity. It has the dimensions of a frequency and can be considered a characteristic frequency of the airplane acceleration response to turbulence.

If the logarithm of both sides of equation (3) is taken, the following relation is obtained:

$$\log N(a_n) = \log N_0 - \frac{a_n^2}{2\sigma^2} \quad (5)$$

Equation (5) indicates that the  $\log N(a_n)$  is a linear function of  $a_n^2$  with slope equal to  $-1/2\sigma^2$ . Thus, for a stationary Gaussian disturbance, the root-mean-square value  $\sigma$  may be obtained simply from the slope of the line for the number of peaks when plotted on semilogarithmic paper as a function of  $a_n^2$ . Because of the linearity of the relationship, this plotting arrangement is found useful.

A representative distribution of the number of peak accelerations per second (both positive and negative peaks) obtained from operations of a transport airplane is shown as the solid curve of figure 4 as a function of  $a_n^2$ . The data are given, as is generally the case, for a threshold value of 0.3g. The distribution appears concave upward and departs considerably from the straight lines that would be expected for a simple stationary Gaussian disturbance in this plot. It is thus clear that the overall distribution of peak accelerations cannot be adequately represented by the simple Gaussian case. A method for obtaining a more adequate representation of the load history is explored in the following paragraphs. For this purpose, the idea of a combination or composite of Gaussian processes is used and equation (2), which

expresses the relation between peak counts and the power spectrum for the simple Gaussian case, is extended to this composite condition.

**Composite Gaussian case.**—If the overall operational load history (in terms of the average number of acceleration peaks per second exceeding given values) is considered to consist of various exposure times to different Gaussian gust disturbances, the average number of peaks per second exceeding given values is given by

$$\overline{M}(a_n) = \sum_{i=1}^k P_i N_i(a_n) \quad (6)$$

where  $P_i$  is the proportion of total flight at the  $i$ th condition and  $N_i(a_n)$  is the number of peak accelerations per second

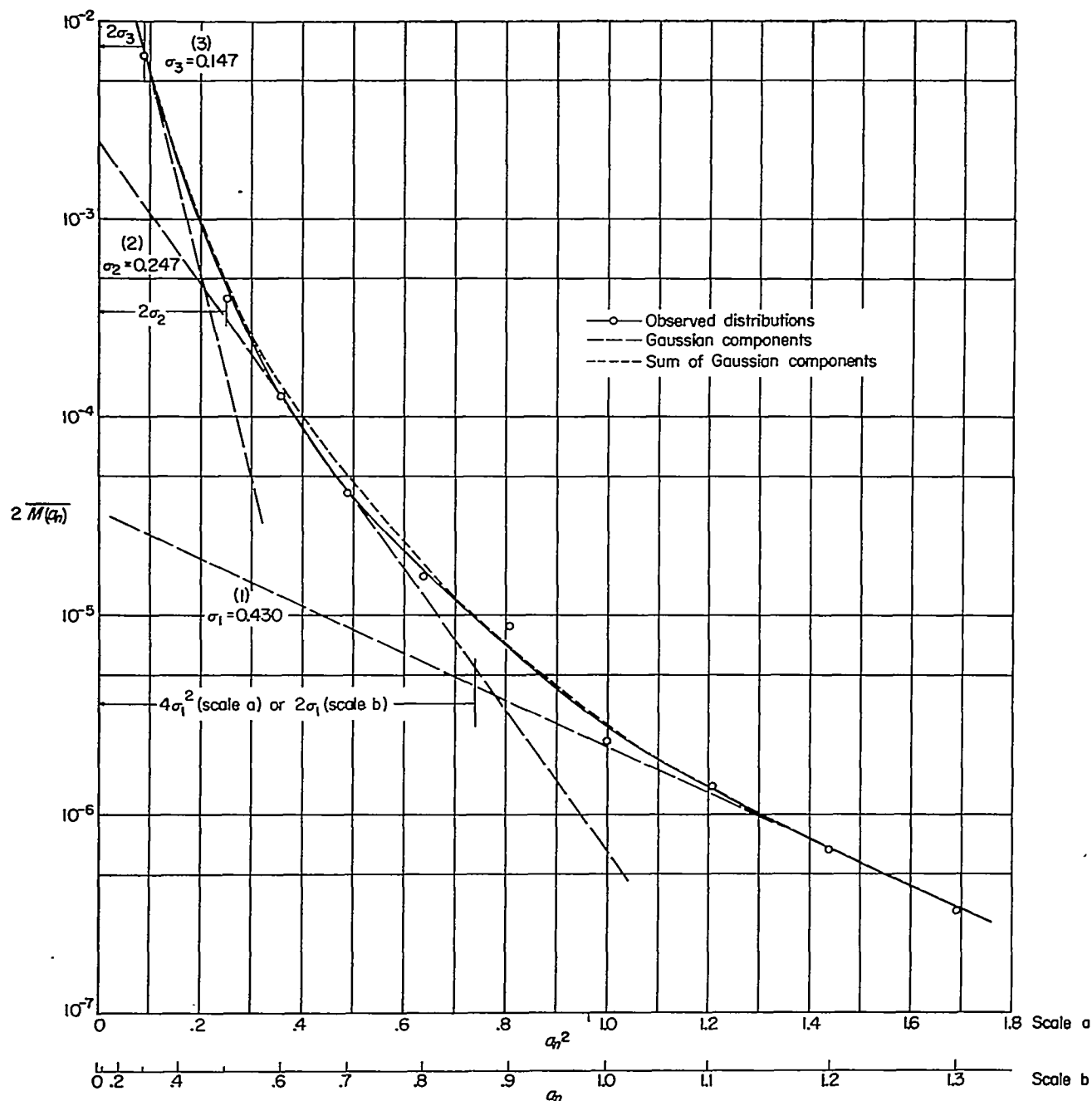


FIGURE 4.—Illustrative example of graphical separation into Gaussian components of distribution of peak acceleration (operation 1).

exceeding given values of acceleration for the  $i$ th condition. In this form, equation (6) is general and permits accounting not only for variation in the spectrum of turbulence but also for variations in the airplane response characteristics.

If equation (3) is substituted into equation (6), there is obtained

$$\overline{M(a_n)} = \sum_{i=1}^k (N_0)_i P_i e^{-a_n^2/2\sigma_i^2} \quad (7)$$

It will be assumed, as previously indicated, that the spectrum of atmospheric turbulence is invariant in shape but varies in intensity or in root-mean-square gust velocity. This assumption is suggested by the available measurements of turbulence spectra and appears reasonable for present purposes. Further, if the response characteristics for a particular airplane in operation are represented by a single-response function, such as obtained for average values of the airplane, and operating parameters, such as the weight, airspeed, and density, equation (7) may be written for this (the discrete) case as

$$\overline{M(a_n)} = N_0 \sum_{i=1}^k P_i e^{-a_n^2/2\sigma_i^2} \quad (8)$$

where the quantity  $N_0$  is, as in equation (3), fixed for a given airplane.

**Continuous case.**—If the airplane is now assumed to encounter turbulence of all intensities (continuous variations in the root-mean-square gust velocity) but of the same spectral shape (fixed value of  $L$  for present applications), equation (8) may be extended for the continuous case to yield the following relation:

$$\overline{M(a_n)} = N_0 \int_0^\infty f(\sigma_{a_n}) e^{-a_n^2/2\sigma_{a_n}^2} d\sigma_{a_n} \quad (9)$$

In this case, the sum of the terms of equation (8) becomes a continuous integral. The expression for the continuous case contains the same characteristic frequency  $N_0$ , which is independent of the turbulence intensity, the same exponential term as the earlier expressions, and, in addition, the function  $f(\sigma_{a_n})$ . This function is the counterpart of the ratios  $P_1, P_2, \dots, P_k$  in equation (8) and is the probability-density distribution of  $\sigma_{a_n}$  which defines the proportion of time spent at various values of  $\sigma_{a_n}$ ; the quantity  $f(\sigma_{a_n})d\sigma_{a_n}$  gives the proportion of flight time spent at values of  $\sigma_{a_n}$  between  $\sigma_{a_n}$  and  $\sigma_{a_n} + d\sigma_{a_n}$ .

The relations between the number of peaks and the root-mean-square values of the random process given by equation (8) for the discrete case and by equation (9) for the continuous case are the basic relations in the present analysis. These two relations are applied in the following sections and methods are developed for estimating the distribution of the root-mean-square acceleration from operational gust-load data generally available in the form of peak counts  $\overline{M(a_n)}$ . Then, the transformation of these distributions of root-mean-square acceleration to distribution of root-mean-square gust velocity is considered.

**DISTRIBUTION OF ROOT-MEAN-SQUARE ACCELERATION FOR DISCRETE CASE**

As previously indicated, the operational load history for a particular airplane in terms of the number of peaks per second exceeding given values is given by equation (8). Each of the terms of the summation of equation (8) is given by

$$\overline{M_i(a_n)} = N_0 P_i e^{-a_n^2/2\sigma_i^2} \quad (10)$$

which, as previously noted, yields a straight line of slope  $-1/2\sigma_i^2$  if  $\log \overline{M(a_n)}$  is plotted as a function of  $a_n^2$ . This condition suggests that the overall operational loads for a given operation when plotted in this specified form can be built up of straight-line or Gaussian components. A simple trial for a sample load history shown in figure 4 indicates that a good approximation to  $\overline{M(a_n)}$  can be obtained with only a few components. (Note that the ordinate of figure 4 is  $2\overline{M(a_n)}$  inasmuch as both acceleration peaks and acceleration minimums have been included in the operational data.) The values for the three components shown add up to give the short-dash curve which is seen to be a close approximation to the overall load history. The procedure devised for the determination of these straight-line components consists of the following steps: First, line (1) is obtained by taking a tangent to the tail of the observed distribution; line (2) is then taken from the point on line (1) which underestimates the observed distribution by one-half and is drawn tangent to the upper part of the overall load-history curve. The third line, if required, is then obtained from line (2) in the same manner that line (2) was obtained from line (1). The sum of the values of the lines obtained in this manner will generally yield a good approximation to the observed distribution, as will be seen subsequently.

The procedure outlined in the preceding paragraph for obtaining the linear components of the observed distribution is somewhat arbitrary. Several alternative procedures were also considered and discarded. These procedures included the selection of the first component at the upper end of the curve and the use of specified combinations of slopes corresponding to given values of root-mean-square gust velocities (which might be considered averages for various weather conditions such as clear-air turbulence and thunderstorms). These alternative procedures appeared to offer no significant advantages and had the additional undesirable characteristic of yielding a poorer approximation at the larger values of acceleration which are of greatest interest.

It will be recalled that the slopes of the lines in figure 4 are equal to  $-1/2\sigma_1^2, -1/2\sigma_2^2,$  and  $-1/2\sigma_3^2$  where  $\sigma_1, \sigma_2,$  and  $\sigma_3,$  respectively, represent the root-mean-square acceleration for the three effective Gaussian components. The values for the case represented in figure 4 are  $\sigma_1=0.430, \sigma_2=0.247,$  and  $\sigma_3=0.147.$  These values  $\sigma_1, \sigma_2,$  and  $\sigma_3$  for the acceleration components are used subsequently to obtain the associated root-mean-square gust velocities for these Gaussian components.

In order to estimate the values of the proportion of total flight time  $P_i$  for the  $i$ th condition, it will be noted from

equation (10) that for each component

$$P_i = \frac{\overline{M_i(a_n)}}{N_0 e^{-a_n^2/2\sigma_i^2}} \quad (11)$$

where  $\overline{M_i(a_n)}$  is the number of accelerations per second exceeding  $a_n$  for the  $i$ th condition or component. The numerator of equation (11) may be obtained directly from the line for each component in figure 4. The denominator of equation (11), as would be expected, is the total number of peak accelerations per second exceeding  $a_n$  that would be experienced if the airplane spent all its flight time at the indicated root-mean-square acceleration value. The value of the denominator is seen to depend upon the value of the constant  $N_0$ .

The values of  $N_0$  and the denominator of equation (11) may be determined in a number of ways. They may be determined from their relation to the power spectrum as given in equations (3) and (4), but this procedure is not very practical for present purposes because the acceleration spectrum cannot be determined from the type of records available. The value of these quantities can also be determined in a number of ways from short sections of flight record in homogeneous rough air. The most direct way is to make use of the property that  $N_0$  is equal to the average number of times per second that  $a_n(t)$  crosses the value zero with positive slope. Unfortunately, the film speed of the records available (2 to 8 feet per hour) was frequently too slow to permit such counts with the desired degree of reliability.

Another method of determining the value of  $N_0$  and the denominator of equation (11) from sample flight records involves the use of the property of equation (3) of defining the average number of peaks or crossings per second above given values of  $a_n$ . If  $a_n$  is set equal to  $k\sigma$  in equation (3), the quantity  $N(k\sigma)$  gives the average number of peaks per second that have a value of  $a_n$  greater than  $k\sigma$  where  $\sigma$  is the value of the root-mean-square acceleration for the record. Thus, from equations (3) and (4)  $N(k\sigma)$ , which is designated as  $N_k$  for brevity, is given by

$$N_k = \frac{1}{2\pi} \left[ \frac{\int_0^\infty \omega^2 \Phi(\omega) d\omega}{\int_0^\infty \Phi(\omega) d\omega} \right]^{1/2} e^{-k^2/2}$$

or

$$N_k = N_0 e^{-k^2/2} \quad (12)$$

Inasmuch as the average number of peaks (or crossings) per second exceeding a value of  $a_n = k\sigma$  can be estimated from the available sample records, equation (12) provides a useful method for determining the value of  $N_0$  and the denominator of equation (11). Care should be taken in such applications to insure that the record section used approximates a Gaussian disturbance.

On this basis, the proportion of flight spent in rough air

yielding a root-mean-square acceleration above  $k\sigma$  is from equation (11) given by

$$P_i = \frac{\overline{M_i(k\sigma_i)}}{N_k} \quad (13)$$

where  $\overline{M_i(k\sigma_i)}$  is the average number of peaks per second exceeding the value  $k\sigma_i$  for the linear component. This relation is used in the subsequent analysis of the operational loads data. In order to avoid the errors associated with the expression for the number of peaks at small values of  $k$ , a value of  $k$  of 2 was generally used. For the illustration of figure 4, the values of  $2\overline{M_1(2\sigma_1)}$ ,  $2\overline{M_2(2\sigma_2)}$ , and  $2\overline{M_3(2\sigma_3)}$  are indicated by ticks on the figure and are  $4.3 \times 10^{-6}$ ,  $3.2 \times 10^{-4}$ , and  $7.4 \times 10^{-3}$ . The sum of the  $P$ 's will in any case be less than one, the remaining time being in either smooth air or very light rough air which does not contribute many peak values above the threshold value.

#### DISTRIBUTION OF ROOT-MEAN-SQUARE ACCELERATION FOR CONTINUOUS CASE

The representation of the load experience in the previous section in terms of a few discrete values of root-mean-square acceleration is a simplification, since atmospheric turbulence may actually be expected to cover a continuous variation in intensity. In this section, the problem of estimating the associated continuous distribution of root-mean-square acceleration from the overall peak counts will be considered.

The determination of the actual probability distribution of root-mean-square acceleration  $f(\sigma)$  from a given peak-load history requires the solution of the integral equation given by equation (9). Since it does not, in general, appear possible to represent the load experience in terms of the number of peak accelerations above given values by a simple function, an effort was made instead to estimate  $f(\sigma)$  directly in simple form, based on the results obtained in the application of the methods for the discrete case. Equation (9) is then integrated and the results obtained are presented in chart form for use in comparison with operational data.

Experience with the analysis of gust-load data, wherein the foregoing discrete-case methods have been used, has indicated that the distribution of  $\sigma$  decreases rapidly with increasing values of  $\sigma$  and might be approximated by simple exponential distributions. On this basis, three exponential-type probability density functions were considered, namely,

$$\left. \begin{array}{l} \text{Case a:} \\ \text{Case b:} \\ \text{Case c:} \end{array} \right\} \begin{array}{l} f_1(\sigma) = \frac{1}{a_1} \sqrt{\frac{2}{\pi}} e^{-\sigma^2/2a_1^2} \\ f_2(\sigma) = \frac{1}{a_2} e^{-\sigma/a_2} \\ f_3(\sigma) = \frac{1}{2a_3^2} e^{-\sqrt{\sigma}/a_3} \end{array} \quad (14)$$

where in each case  $\sigma \geq 0$ .



For each case,  $a$  is a scale parameter, larger values of  $a$  representing more severe load histories. The three distributions are shown in figure 5 for values of  $a=1$  and, in order, are seen to have increasingly larger areas at the higher values of  $\sigma$ . These functions, by the definition of a probability density function, all have unit area.

Case a.—If it is assumed that  $f(\sigma)$  is given by case a, equation (9) may be integrated in closed form and yields the following result for  $\overline{M}(a_n)/N_0$ :

$$\frac{\overline{M}(a_n)}{N_0} = e^{-a_n/a_1} \quad (15)$$

The function  $\overline{M}(a_n)/N_0$  gives the proportion of peak accelerations exceeding given values of  $a_n$  and is thus a cumulative probability distribution. Figure 6(a) shows the distribution  $\overline{M}(a_n)/N_0$  for a range of values of  $a_1$ . Equation (15) yields a simple result for the proportion of peak accelerations per second exceeding given values of  $a_n$ , in terms of the single-scale parameter of the distribution of  $\sigma_{a_n}$ . The value of the parameter  $a_1$  is inversely proportional to the slope of the line for  $\overline{M}(a_n)/N_0$  when plotted on semilogarithmic paper and also gives the value of  $\sigma_{a_n}$  below which 68 percent of the airplane flight time is spent. The linear variation with  $a_n$  of the  $\log \overline{M}(a_n)$  given by equation (15) is of considerable interest because gust-load flight-test data on peak accelerations under some conditions, particularly where a limited range of weather conditions is represented, tend to exhibit linear trends when plotted on semilogarithmic paper ( $\log \overline{M}(a_n)$  as a function of  $a_n$ ). This condition, however, does not generally apply to operational data.

Case b.—The distributions of  $\overline{M}(a_n)$  observed from operational flights frequently exhibit a nonlinear trend and

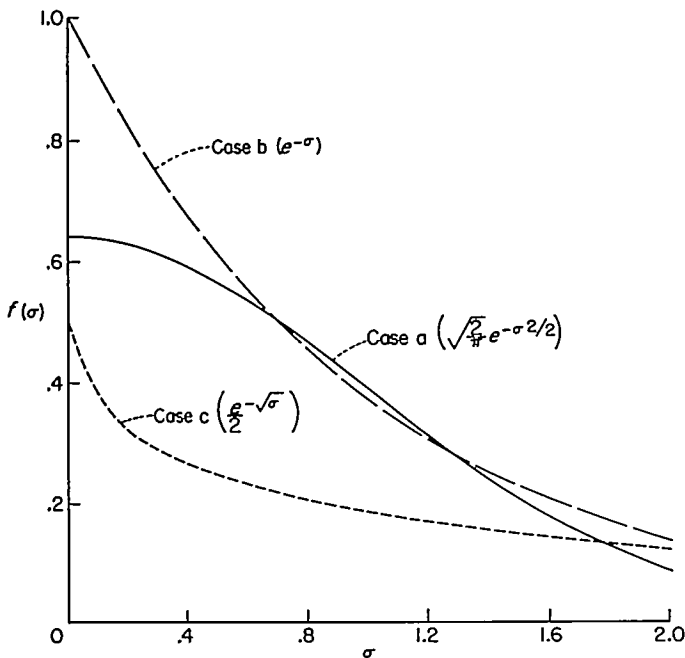


FIGURE 5.—Comparison of three assumed distributions.

a concave upward form when the  $\log \overline{M}(a_n)$  is plotted against  $a_n$ . This form implies that the distributions of  $f(\sigma)$  for these cases might more adequately be represented by case b or case c. Substituting the expression for case b in equation (9) yields the following expression for the number of maximums exceeding  $a_n$ :

$$\overline{M}(a_n) = \int_0^\infty \frac{N_0}{a_2} e^{-\frac{a_n^2}{2\sigma^2} \frac{\sigma}{a_2}} d\sigma \quad (16)$$

A closed-form evaluation of the integral could not be found. Numerical evaluations of the integral, however, are made readily. If the substitution  $\sigma = sa_2$  is made into equation (16) and both sides of the equation are divided by  $N_0$ , the following result is obtained:

$$\frac{\overline{M}(a_n)}{N_0} = \int_0^\infty e^{-\frac{a_n^2}{2a_2^2} \frac{1}{s^2}} ds \quad (17)$$

Equation (17) was evaluated for various values of  $a_n^2/2a_2^2$  so that  $\overline{M}(a_n)/N_0$  could be determined for various values of  $a_2$ . The results obtained are shown plotted in figure 6(b). Operational gust-load data can be plotted conveniently in figure 6(b) in order to determine whether they adhere to the present distribution shape and, if so, to obtain the appropriate value of the scale parameter  $a_2$ . (The plotting requires the determination of the value of  $N_0$  which may be estimated from flight records as described previously.) The points shown in the figure represent operational gust-load data which are discussed in a subsequent section.

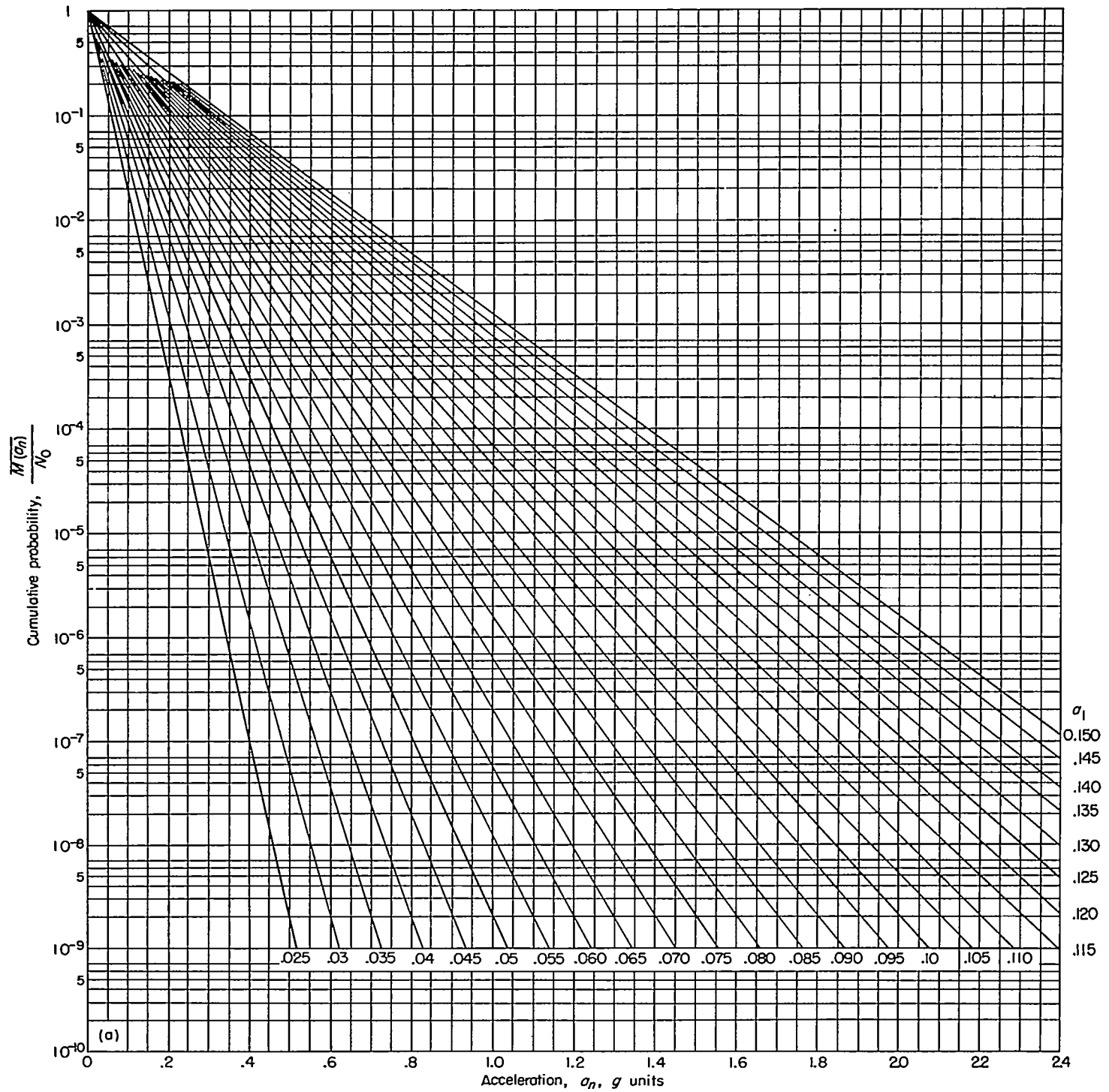
Case c.—For case c, equation (9) becomes

$$\frac{\overline{M}(a_n)}{N_0} = \frac{1}{2a_3^2} \int_0^\infty e^{-\frac{a_n^2}{2\sigma^2} \frac{\sqrt{\sigma}}{a_3}} d\sigma \quad (18)$$

Equation (18) could not be evaluated in closed form but was evaluated numerically for various values of  $a_3$ . The results obtained for a range of values of  $a_3$  are shown in figure 6(c). Operational gust-load data can also be plotted conveniently in figure 6(c) in order to determine whether they adhere to the present distribution shape and, if so, to obtain the appropriate value of the parameter  $a_3$ .

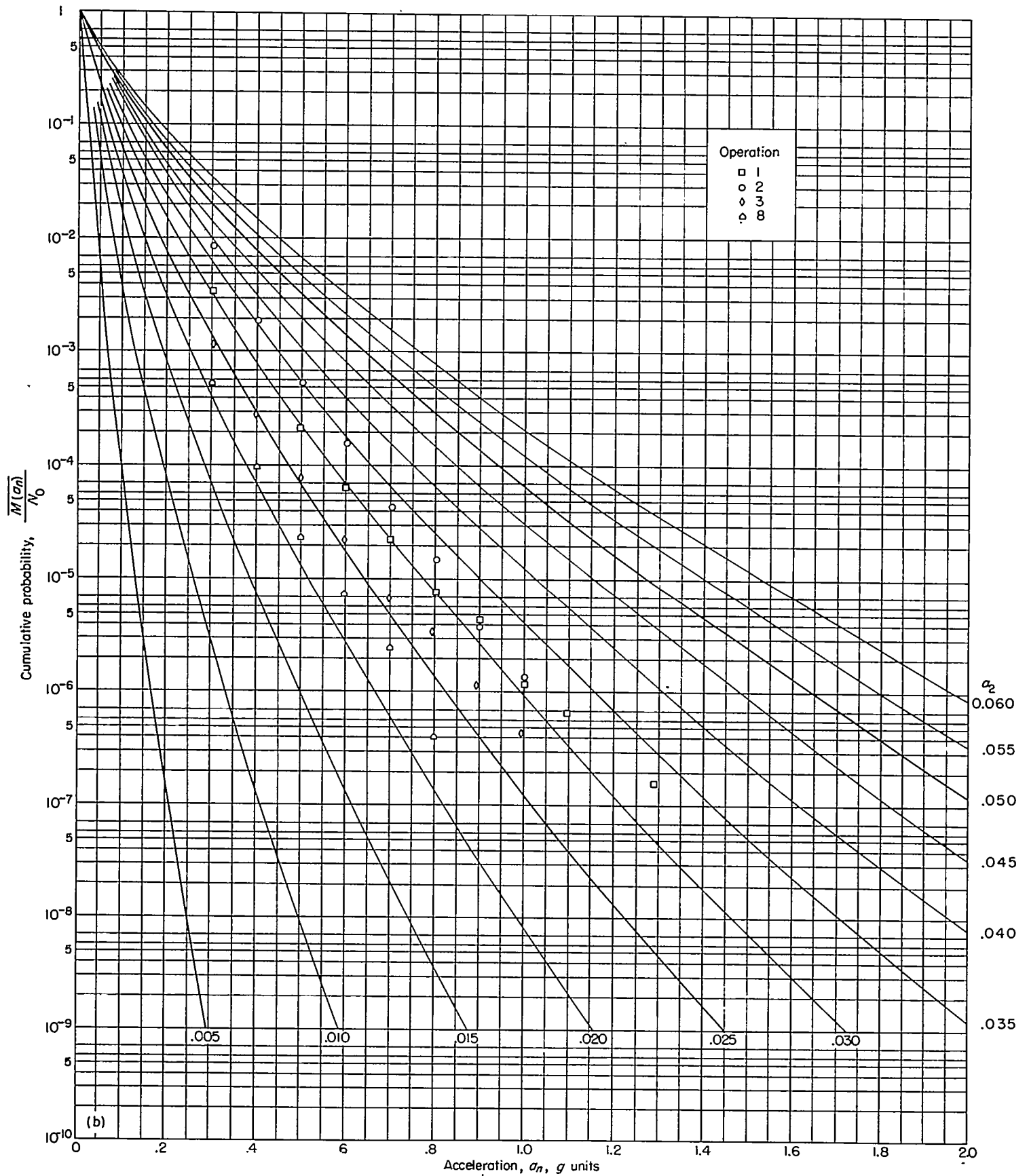
In general, a good representation of the observed distribution of peak values can be obtained by comparison of the data with the three charts of figure 6.<sup>2</sup> The choice of the appropriate case and the value of the scale parameter then specify the probability distribution of the root-mean-square acceleration in accordance with equations (14). As will be seen in the section entitled "Application to Gust-Load Statistical Data," these three distributions appear, in most cases, to be adequate for the representation of the types of data so far considered. However, other distribution forms appear worth investigating in future studies.

<sup>2</sup> The charts of figures 6(b) and 6(c) contain extensions and revisions to the charts presented earlier in Technical Note 3362.



(a) Case a.

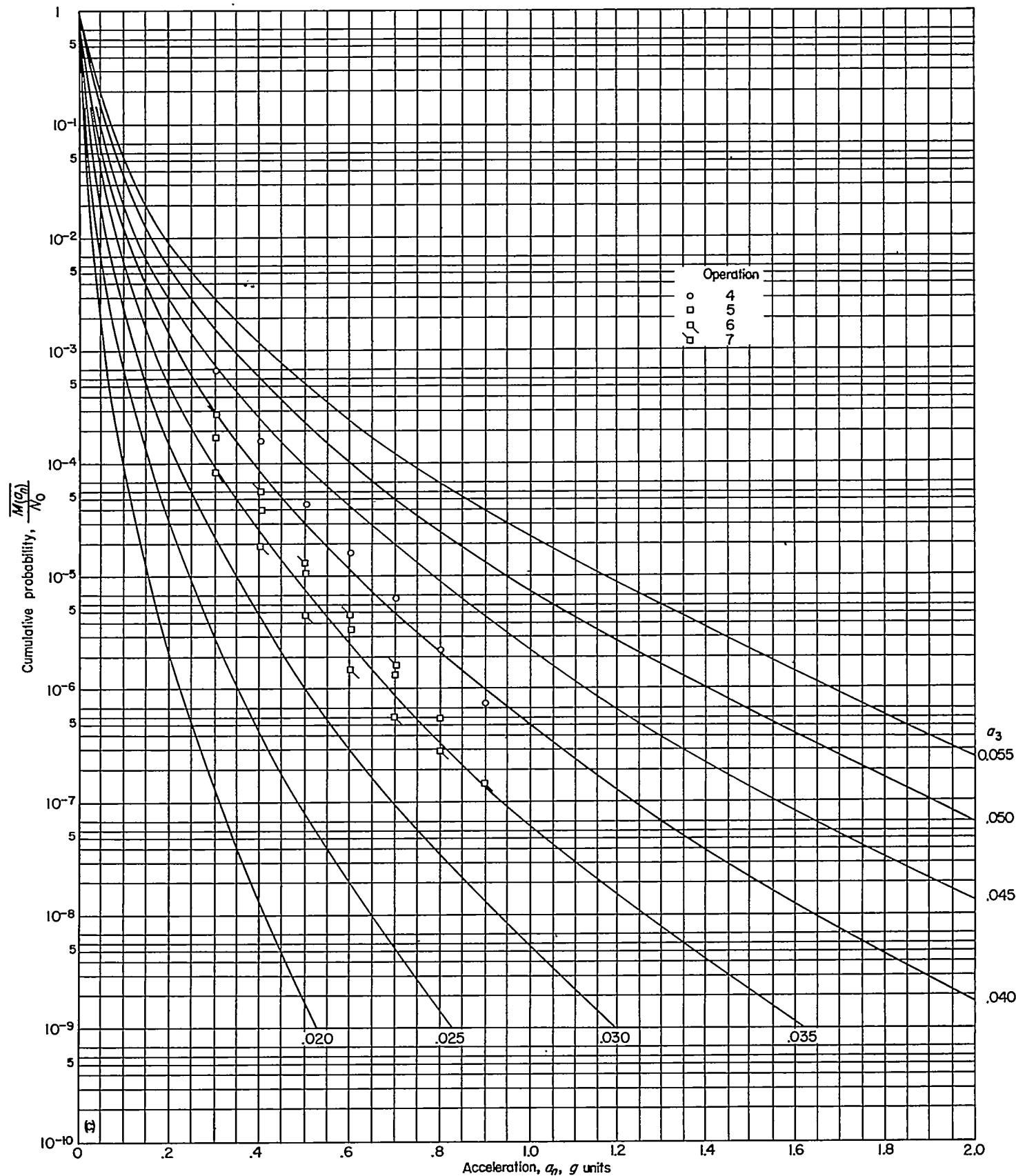
FIGURE 6.—Cumulative probability of a peak acceleration exceeding given values of  $a_n$ .



(b)

(b) Case b.

FIGURE 6.—Continued.



(c) Case c.

FIGURE 6.—Concluded.

**DISTRIBUTION OF ROOT-MEAN-SQUARE GUST VELOCITY**

In the foregoing sections, methods have been given for converting the overall load histories from counts of peak accelerations into several discrete root-mean-square values of acceleration and their associated percentage exposure times to each level or into a continuous distribution of root-mean-square acceleration. The problem of the conversion of these results into the airplane gust experience is now considered.

The root-mean-square gust acceleration in rough air is related to the turbulence spectrum and the airplane response characteristics by the following equation:

$$\begin{aligned} \sigma_{a_n}^2 &= \int_0^\infty \Phi_{v(\omega)} T^2(\omega) d\omega \\ &= \int_0^\infty \Phi_{a_n}(\omega) d\omega \end{aligned} \quad (19)$$

where  
 $\Phi_{v(\omega)}$  power spectrum of vertical gust velocity  
 $T(\omega)$  amplitude of airplane acceleration response to sinusoidal gusts of unit amplitude  
 $\Phi_{a_n}(\omega)$  power spectrum of airplane normal acceleration

Since the root-mean-square acceleration obtained by the preceding evaluation is seen to depend on both the spectrum of turbulence and the airplane response characteristics, the root-mean-square acceleration is apparently not sufficient to fix the turbulence spectrum. Several procedures appear possible for the analysis of load measurements for the present purpose of deducing root-mean-square gust velocities. These include the actual measurement of acceleration spectra and the calculation of the airplane frequency-response function. The turbulence spectrum is then given by

$$\Phi_{v(\omega)} = \frac{\Phi_{a_n}(\omega)}{T^2(\omega)} \quad (20)$$

This procedure is extremely laborious and requires extensive calculations for the output spectrum  $\Phi_{a_n}(\omega)$ ; the reliability of the results, in turn, depends upon the reliability of the calculated airplane transfer functions. At the present time, it is unlikely that the large amount of work involved in this approach is warranted even if the available records were in a form which would permit this type of analysis. Actually, the film speed used for the available records was far too slow to permit this type of analysis.

As an alternative, some simplifications appear warranted. As a preliminary effort in this direction, it will be assumed that:

- (1) The airplane is rigid.
- (2) The airplane is free to move vertically only (not pitch.)
- (3) The spectrum of vertical gust velocity is given by

$$\Phi_{v(\Omega)} = \sigma_v^2 \frac{L}{\pi} \frac{1+3\Omega^2 L^2}{(1+\Omega^2 L^2)^2}$$

where  $\Omega$  is a reduced frequency  $\omega/V$  in radians per foot and  $L$  is the scale of turbulence.

These assumptions, although crude, should nevertheless provide some reasonable approximations of the gust histories. The possible magnitude of the errors introduced by these assumptions is considered in the section entitled "Reliability of Results."

For the foregoing conditions, a useful result obtained by Y. C. Fung (ref. 2) is that

$$\bar{Z}^2 = \sigma_v^2 \frac{16V^2}{\pi \bar{c}^2 (1+K)^2} I(K, s) \quad (21)$$

where

$\bar{Z}^2$  mean-square acceleration  
 $\bar{c}$  mean chord  
 $K$  airplane mass parameter,  $\frac{4W}{g\pi\rho S\bar{c}}$   
 $s$  ratio of mean chord to scale of turbulence,  $\bar{c}/L$   
 Since  $K \gg 1$  in almost all cases of concern, equation (21) may be simplified to yield

$$\begin{aligned} \sigma_{a_n} &= \sigma_v \frac{\rho V S m}{2W} \sqrt{\frac{I(K, s)}{\pi}} \\ \sigma_{a_n} &= \bar{A}_1 \sigma_v \end{aligned} \quad (22)$$

where

$$\bar{A}_1 = \frac{\rho V S m}{2W} \sqrt{\frac{I(K, s)}{\pi}}$$

and  $\sqrt{\frac{I(K, s)}{\pi}}$  is an airplane gust-response factor defined in reference 2 and is shown in figure 7 as a function of  $K$  for various values of  $s = \bar{c}/L$ .

In this representation, the three-dimensional slope of the lift curve  $m$  has been used to replace  $2\pi$  in order to account for the overall three-dimensional aerodynamic effects. In this form, observed values of  $\sigma_{a_n}$  may be used directly with the values of the airplane parameters to determine  $\sigma_v$ . This calculation requires the determination of the value of  $\bar{A}_1$ . For this purpose, it would appear adequate to use average values of  $\rho$ ,  $V$ , and  $W$  as well as an average value of  $K$  for a given operation or, if greater precision is required, for portions of an operation. Thus, the quantity  $\bar{A}_1$  may be treated as a constant for a given operation (or portion of an operation).

It should be noted that the direct proportionality between the root-mean-square gust velocity and acceleration as given by equation (22) is not restricted to the one-degree-of-freedom case but may be generalized to cover as many degrees of freedom as desirable. In general,

$$\sigma_{a_n} = \bar{A} \sigma_v \quad (22a)$$

where, from equation (19),  $\bar{A}$  is defined by

$$\bar{A} = \frac{1}{\sigma_v} \left[ \int_0^\infty \Phi_{v(\Omega)} T^2(\Omega) d\Omega \right]^{1/2} \quad (22b)$$

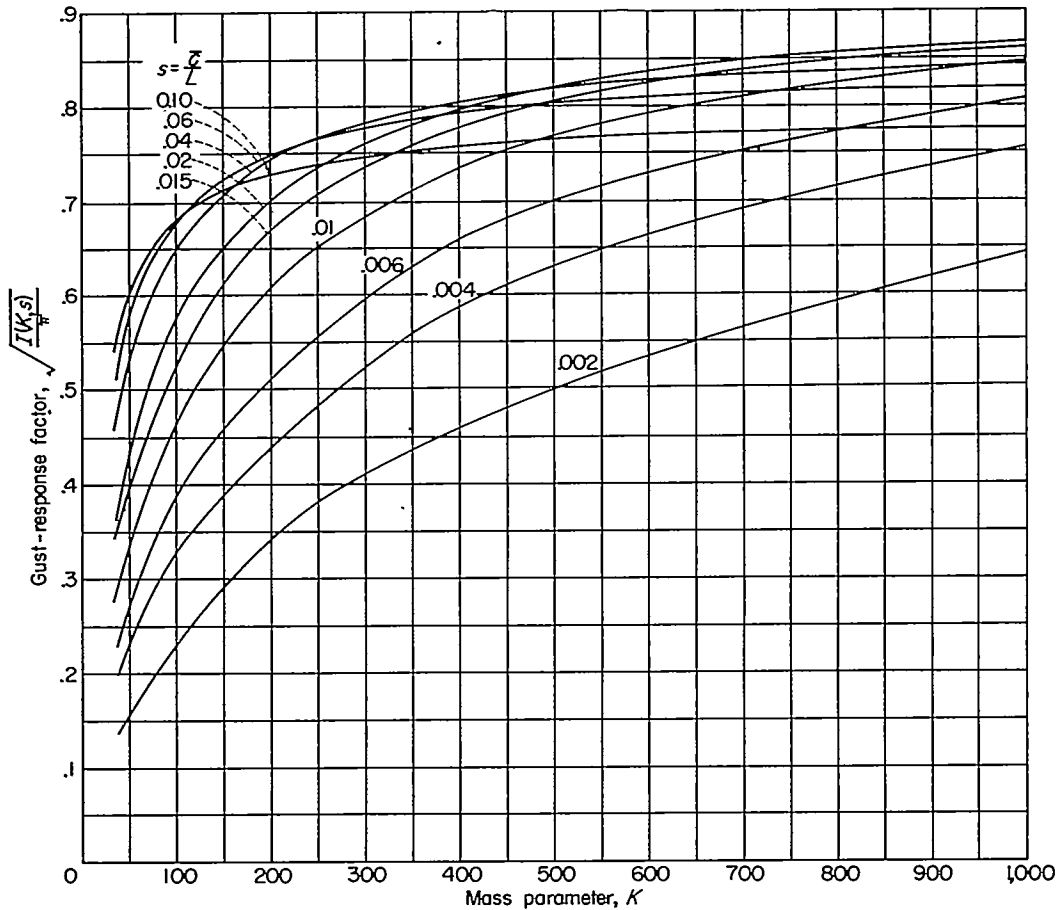


FIGURE 7.—Gust-response factor  $\sqrt{\frac{I(K,s)}{\pi}}$ .

or for the gust spectrum assumed herein

$$\bar{A} = \left[ \frac{L}{\pi} \int_0^\infty \frac{1+3\Omega^2 L^2}{(1+\Omega^2 L^2)^2} T^2(\Omega) d\Omega \right]^{1/2} \quad (22c)$$

In these cases, the amplitude of the airplane frequency response function  $T(\Omega)$  will depend upon additional aerodynamic, geometric, and structural parameters of the airplane rather than upon those considered in the single-degree-of-freedom case.

For the case of discrete values of  $\sigma_{a_n}$ , equation (22) permits the direct evaluation of the associated values of root-mean-square gust velocity  $\sigma_V$  for the single-degree-of-freedom case.

For the case of a continuous distribution of root-mean-square acceleration, the appropriate distribution of root-mean-square gust velocity is obtained from equation (22) or (22a) by the relation for a change of variables for probability distributions and in terms of  $f(\sigma_{a_n})$  is given by

$$\hat{f}(\sigma_V) = \bar{A}_1 f(\bar{A}_1 \sigma_V) \quad (\sigma_{a_n} = \bar{A}_1 \sigma_V) \quad (23a)$$

$$\hat{f}(\sigma_V) = \bar{A} f(\bar{A} \sigma_V) \quad (\sigma_{a_n} = \bar{A} \sigma_V) \quad (23b)$$

Thus, for the three acceleration distributions considered, the distributions of root-mean-square gust velocity are given by the following equations:

Case a:

$$\hat{f}_1(\sigma_V) = \frac{1}{b_1} \sqrt{\frac{2}{\pi}} e^{-\sigma_V^2/2b_1^2}$$

where

$$b_1 = \frac{a_1}{\bar{A}_1}$$

Case b:

$$\hat{f}_2(\sigma_V) = \frac{1}{b_2} e^{-\sigma_V/b_2}$$

where

$$b_2 = \frac{a_2}{\bar{A}_1}$$

Case c:

$$\hat{f}_3(\sigma_V) = \frac{1}{2b_3^3} e^{-\sqrt{\sigma_V}/b_3}$$

where

$$b_3 = \frac{a_3}{\sqrt{\bar{A}_1}}$$

(24)

**DIRECT TRANSFER OF GUST LOADS FROM ONE AIRPLANE TO ANOTHER**

It may on occasion be desirable to transfer the gust loads directly from one airplane to another without recourse to first determining the probability distributions of root-mean-square acceleration and gust velocity. The following analysis indicates a simple direct manner of performing this transfer.

Consider airplanes *i* and *j*. Assume that the gust loads have been measured on airplane *i* under fixed operating conditions and that it is desired to determine the load experience for airplane *j* under fixed operating conditions and with the same turbulence experience as that of airplane *i*. For airplane *i*,

$$\overline{M_i(a)} = (N_0)_i \int_0^\infty f_i(\sigma_i) e^{-a^2/2\sigma_i^2} d\sigma_i \quad (25)$$

where the subscripts for acceleration have been omitted for brevity. Similarly, for airplane *j*

$$\overline{M_j(a)} = (N_0)_j \int_0^\infty f_j(\sigma_j) e^{-a^2/2\sigma_j^2} d\sigma_j \quad (26)$$

If the turbulence experience is the same for both airplanes, then

$$\sigma_j = \frac{\overline{A_j}}{\overline{A_i}} \sigma_i \quad (27)$$

by virtue of equation (22) or (22a). Substituting equation (27) into equation (26) and making use of the relation for the change of variables for probability distributions yields

$$\overline{M_j(a)} = (N_0)_j \int_0^\infty f_i(\sigma_i) e^{-\left(\frac{a\overline{A_i}}{\overline{A_j}}\right)^2 / 2\sigma_i^2} d\sigma_i \quad (28)$$

The integral on the right-hand side is, from equation (25), equal to the quantity

$$\overline{M_i\left(\frac{\overline{A_i}}{\overline{A_j}} a\right)} / (N_0)_i \quad (29)$$

Thus,

$$\overline{M_j(a)} = \frac{(N_0)_j}{(N_0)_i} \overline{M_i\left(\frac{\overline{A_i}}{\overline{A_j}} a\right)} \quad (30)$$

Equation (30) indicates that, in order to obtain the load history  $\overline{M_j(a)}$ , it is only necessary to take the value of measured distribution  $\overline{M_i(\quad)}$  at the acceleration value  $\left(\frac{\overline{A_i}}{\overline{A_j}} a\right)$  and multiply the result by the ratio of the characteristic frequencies  $(N_0)_j / (N_0)_i$ . Essentially, the operation involves only a change of the abscissa scale and a multiplication of the ordinate value by the ratio of the characteristic frequencies.

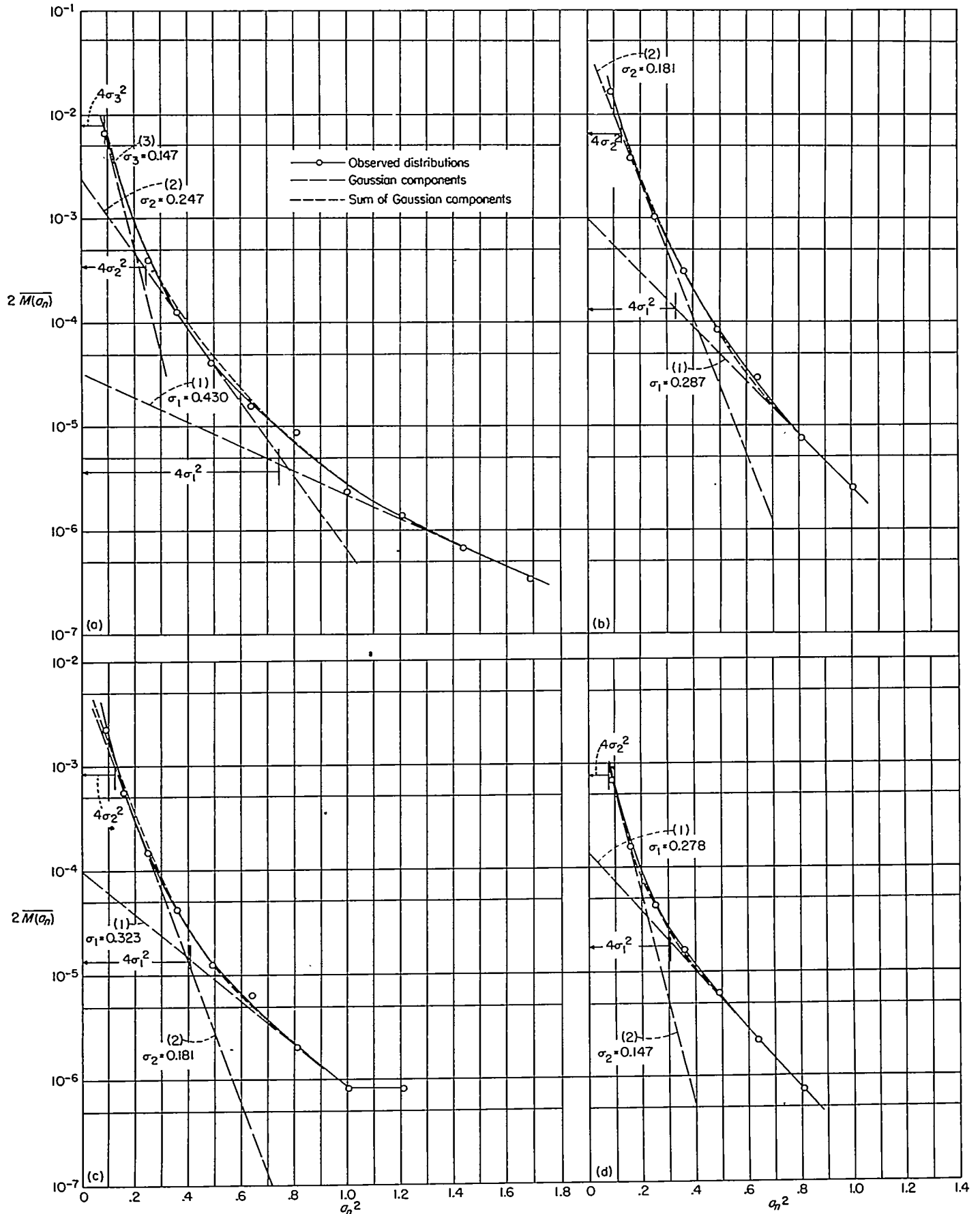
It should be noted that the values of  $\overline{A}$  need not necessarily be restricted to the one-degree-of-freedom case considered in the present conversion of the acceleration data to gust velocities. In many cases, it may be desirable to consider a more complete dynamic analysis in determining the quantities  $N_0$  and  $\overline{A}$ .

**APPLICATION TO GUST-LOAD STATISTICAL DATA**

In this section, the methods developed in the section on derivation of conversion techniques are applied to available gust-load statistical data in order to convert the statistical data in terms of peak counts of accelerations and gusts into distribution of root-mean-square gust velocity. The data to be considered are of two types: first, data obtained from a number of different transport operations, and, then, in order to obtain a description of the turbulence that is more flexible than the operational gust experience and that is applicable to arbitrary flight plans, available data on the variation of turbulence with altitude and with weather condition. For the operational data, both the discrete and continuous methods are applied; whereas, only the continuous case is considered for the other data.

**OPERATIONAL GUST-LOAD HISTORIES**

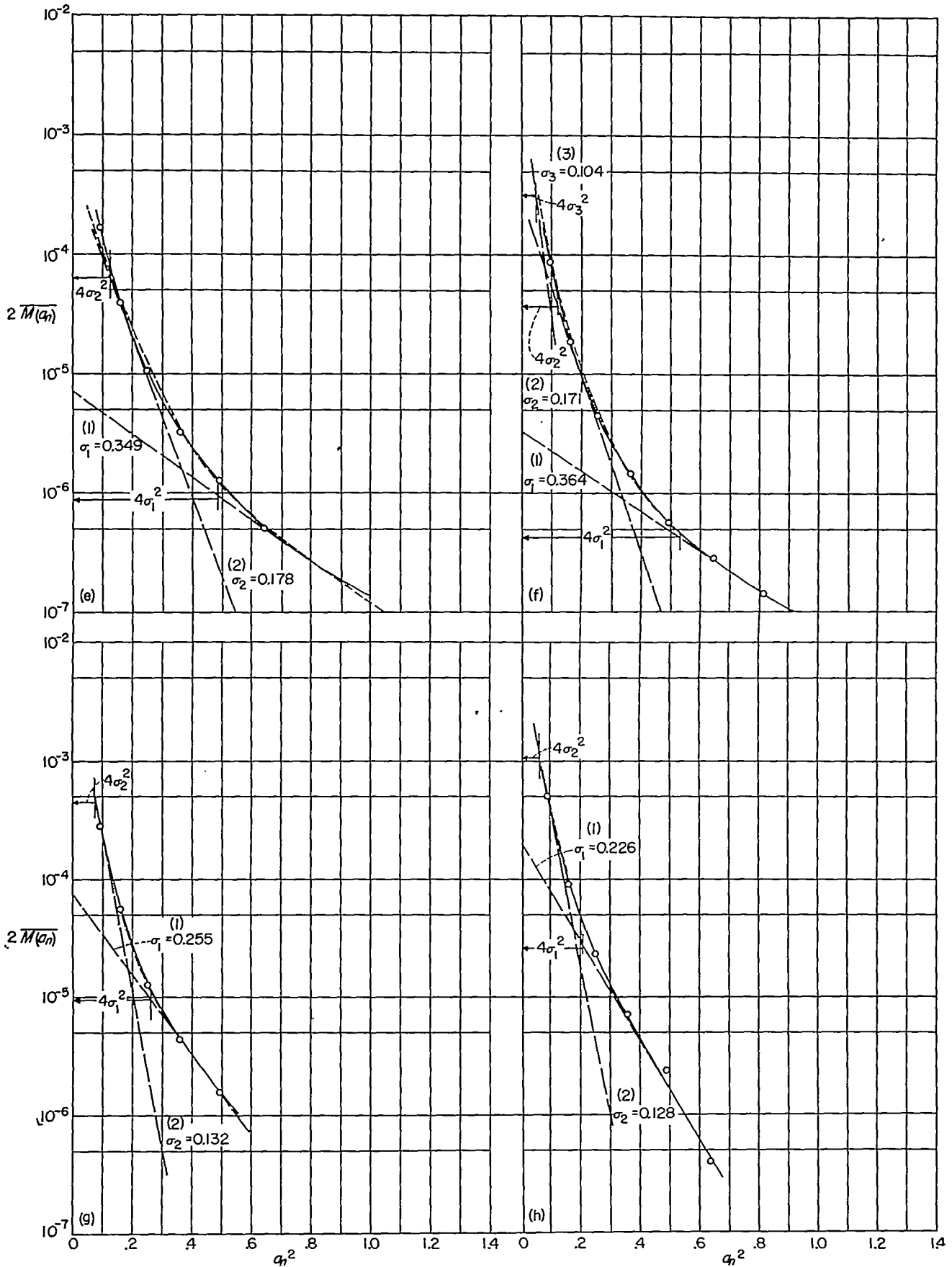
**Discrete case.**—The graphical procedure outlined in an earlier section is applied to a series of eight operational load histories obtained from NACA VGH records. The scope of the data considered is summarized in table I. The data were obtained from six different types of transport airplanes with operations 5, 6, and 7 representing the same airplane type flown by different operators. The pertinent airplane characteristics and operating conditions are given in table II. These data include estimates of the overall average flight altitude, average flight speed, and average weight. The overall distributions of peak accelerations measured in flight are given in table III. Because of the limited data available, no effort was made to consider breakdowns of the overall data by flight condition or altitude. Values of  $N_0$  and  $N_s$ , given in table IV, were estimated in accordance with equation (12) from sections of record obtained in continuous rough air by counting the number of peak accelerations exceeding  $2\sigma$ . These values contain some revisions of the values presented earlier in NACA Technical Note 3362 but owing to the nature of the records available are still considered crude estimates. The measured distributions of acceleration increments for the eight operations are shown in figures 8 (a) to 8 (h). (The illustration previously considered in figure 4 is operation 1 which is also shown in fig. 8 (a).) The subdivision of the distribution into Gaussian components in the manner previously described is also indicated by the long-dash lines in each case. The values of  $\sigma_i$  and  $P_i$  for each operation obtained from the slopes of the linear components and the values of  $2\overline{M}(2\sigma_i)$  were determined in each case and are summarized in table IV.



(a) Operation 1. (b) Operation 2.  
 (c) Operation 3. (d) Operation 4.

FIGURE 8.—Graphical separation into Gaussian components of distribution of peak acceleration.





(e) Operation 5.  
 (g) Operation 7.

(f) Operation 6.  
 (h) Operation 8.

FIGURE 8.—Concluded.

The results of figure 8 and table IV indicate that the operational load histories can, in most cases, be reproduced by numbers of the order of 1 percent of the flight time at  $\sigma_{a_n}=0.15g$  and 0.05 percent of the flight time at  $\sigma_{a_n}=0.3g$ . In some cases, three components were found desirable. Actually, the total flight time in rough air is considerably higher than the 1 percent indicated by these values, as previously mentioned, and should perhaps include as much as 10 percent at a lower value of  $\sigma_{a_n}$  of the order of 0.05g. This flight time would yield the primary contribution to the number of peak accelerations at values of  $a_n$  below 0.3g but contributes only a few peak accelerations above the threshold value of 0.3g used in the data evaluations considered herein.

The conversion of the root-mean-square accelerations to root-mean-square gust velocities requires the determination of the value of the quantity  $\bar{A}_1$  for each operation, as defined in equation (22),

$$\bar{A}_1 = \frac{\rho V S m}{2W} \sqrt{\frac{I(K,s)}{\pi}}$$

For this purpose, the airplane characteristics given in table II were used along with the average values of air density, airspeed, and airplane weight. In determining the gust response factor, average values of weight and air density were also used along with a value of  $L$  of 1,000 feet. The values of  $\bar{A}_1$  obtained for the eight operations and the resultant values obtained for  $\sigma_V$  are given in table IV. It is of interest to note that a change in the value of  $L$  by a factor of 2 results in root-mean-square gust velocities that are increased by about 25 percent if  $L$  is doubled ( $L=2,000$  feet) or decreased by about 25 percent if  $L$  is halved ( $L=500$  feet).

**Continuous case.**—In order to determine the appropriate continuous distribution of root-mean-square acceleration, the tabulated distributions of table III were compared with curves of figure 6. Operations 1, 2, 3, and 8 appeared to follow case b best and are shown in figure 6 (b). (The measured distribution of peaks which included positive and negative peaks was divided by 2 for this comparison.) The appropriate values of  $a_2$  can be obtained from the figure by interpolation and are given in table IV. The distribution of  $\sigma_a$  for these operations is, from equations (14), given by

$$f_2(\sigma_a) = \frac{1}{a_2} e^{-\sigma_a/a_2} \quad (\sigma \geq 0)$$

It is of interest to note that all three of the two-engine aircraft in low-altitude operations, operations 1, 2, and 3, are best represented by this case.

The remaining four operations had a slower rate of decrease in  $\bar{M}(a_n)/N_0$  with increasing  $a_n$ ; this condition suggested that case c might be more appropriate. The data for these operations are shown plotted in figure 6 (c) and are in fair agreement with the curves for case c. Again, one-half the measured distributions are plotted to be comparable with

the calculated curves. The acceleration histories for these operations are thus described by the probability distribution for case c (eqs. (14))

$$f_3(\sigma_a) = \frac{1}{2a_3^2} e^{-\sqrt{\sigma_a}/a_3}$$

where the appropriate value of  $a_3$  determined by interpolation from figure 6 (c) for each operation is given in table IV.

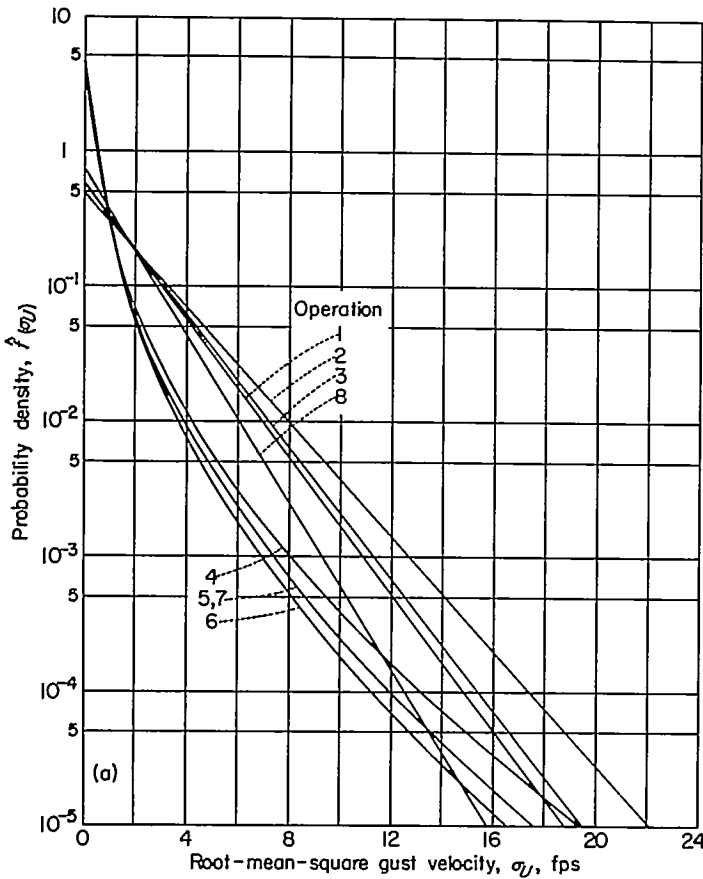
In some of the foregoing cases, the acceleration histories are not too well represented by the analysis. Better representations, if desirable, can be obtained, however, by considering combinations of the three distributions or more complicated distribution forms.

The conversion of these distributions to distributions of root-mean-square gust velocities only requires the determination of the values of  $b$  defined in equations (24). The appropriate values of  $b$  ( $b_2$  or  $b_3$ ) were determined by use of the values of  $\bar{A}_1$  for each operation and are given in table IV. These values apply to the associated distributions which are given by equations (24). The probability distributions obtained for each of the operations are shown in figure 9 (a). Because of the changes in the values of  $N_0$  and several other minor changes, these results also differ in some cases from those presented in NACA Technical Note 3362. The cumulative probability distributions, which are obtained by integrating the probability distributions, are given in figure 9 (b) and define the proportion of total flight time spent in turbulence exceeding given values of  $\sigma_V$ .

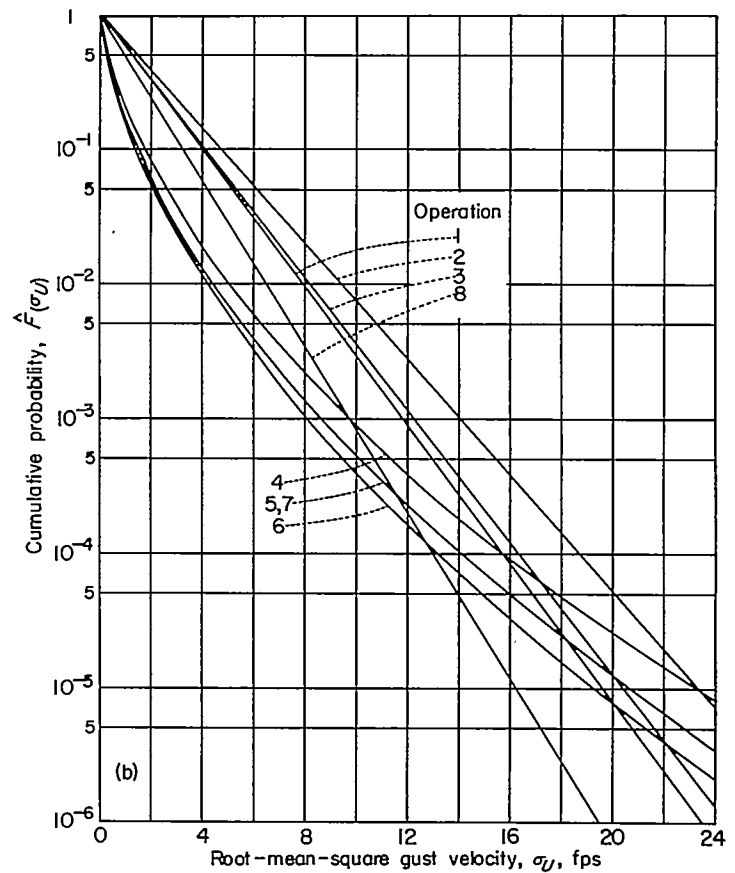
The description of the gust experience in this form is directly applicable to load calculations for other airplanes in similar operations by reversing the procedures used in obtaining these results. However, direct application of these results would apply only to similar operations. In order to obtain results that are more flexible and applicable to arbitrary flight plans, it would be desirable to determine the variations in these distributions with altitude, weather condition, and, perhaps, geography. Preliminary results obtained in this respect are described in the next sections.

#### VARIATION WITH ALTITUDE

**Conversion of data.**—In order to arrive at some rough estimates of the variation of  $\hat{f}(\sigma_V)$  with altitude, use was made of the summary of gust statistics given in reference 22. Figure 6 of reference 22 presents estimates of the average gust experience at various altitudes that are representative of contemporary types of transport operations. In order to estimate the associated distributions of root-mean-square gust velocity, these results which are in terms of the frequencies of derived gust velocities were, for convenience, first converted to acceleration peaks by using the conventional gust-response equation as given, for example, in reference 12, and the characteristics of a representative transport airplane. The charts of figure 6 could then be used to estimate the appropriate distribution form and the scale value  $a$ .



(a) Probability density.



(b) Cumulative probability.

FIGURE 9.—Probability distribution of the root-mean-square gust velocity for eight operations.

The airplane and operating parameters used for this conversion to accelerations are given in table V. The acceleration histories as defined by the cumulative probability distribution of peak accelerations  $\overline{M}(a_n)/N_0$  obtained on this basis are shown in figure 10 (a) for each 10,000-foot altitude bracket with the exception of the lowest altitude bracket. Also shown in the figure are curves for  $\overline{M}(a_n)/N_0$  corresponding to the probability distribution of root-mean-square acceleration  $f_3(\sigma_{a_n})$  as given in figure 6 (c). It will be noted that, except for the lowest altitude bracket, the acceleration histories can be reasonably well approximated by members of this family of distributions. The appropriate values of  $a_3$  obtained by interpolation on the figure for these altitudes are given in table V. For the lowest altitude bracket, 0 to 10,000 feet, a better representation was needed. A few trials indicated that a very good approximation for the data for the lowest altitude bracket could be obtained by the following two-term probability distribution:

$$f(\sigma_{a_n}) = (0.99) \frac{1}{0.026} e^{-\sigma_{a_n}/0.026} + (0.01) \frac{1}{0.050} e^{-\sigma_{a_n}/0.050} \quad (31)$$

The distribution of peak accelerations  $\overline{M}(a_n)/N_0$  corresponding to this distribution for  $\sigma_{a_n}$  is shown in figure 10 (b) as the short-dash curve and is seen to be in excellent agreement with the data points for this altitude bracket. The contribution

of each of the two terms of the right-hand side of equation (31) to the total curve is indicated by the two long-dash curves.

By applying the values of  $\overline{A}_1$  for each altitude bracket in table V and the foregoing results in equation (23a), the following distributions  $\hat{f}(\sigma_v)$  were obtained for the various altitude brackets:

For the altitude bracket of 0 to 10,000 feet,

$$\hat{f}(\sigma_v) = 0.99 \frac{1}{1.48} e^{-\sigma_v/1.48} + 0.01 \frac{1}{2.84} e^{-\sigma_v/2.84} \quad (32)$$

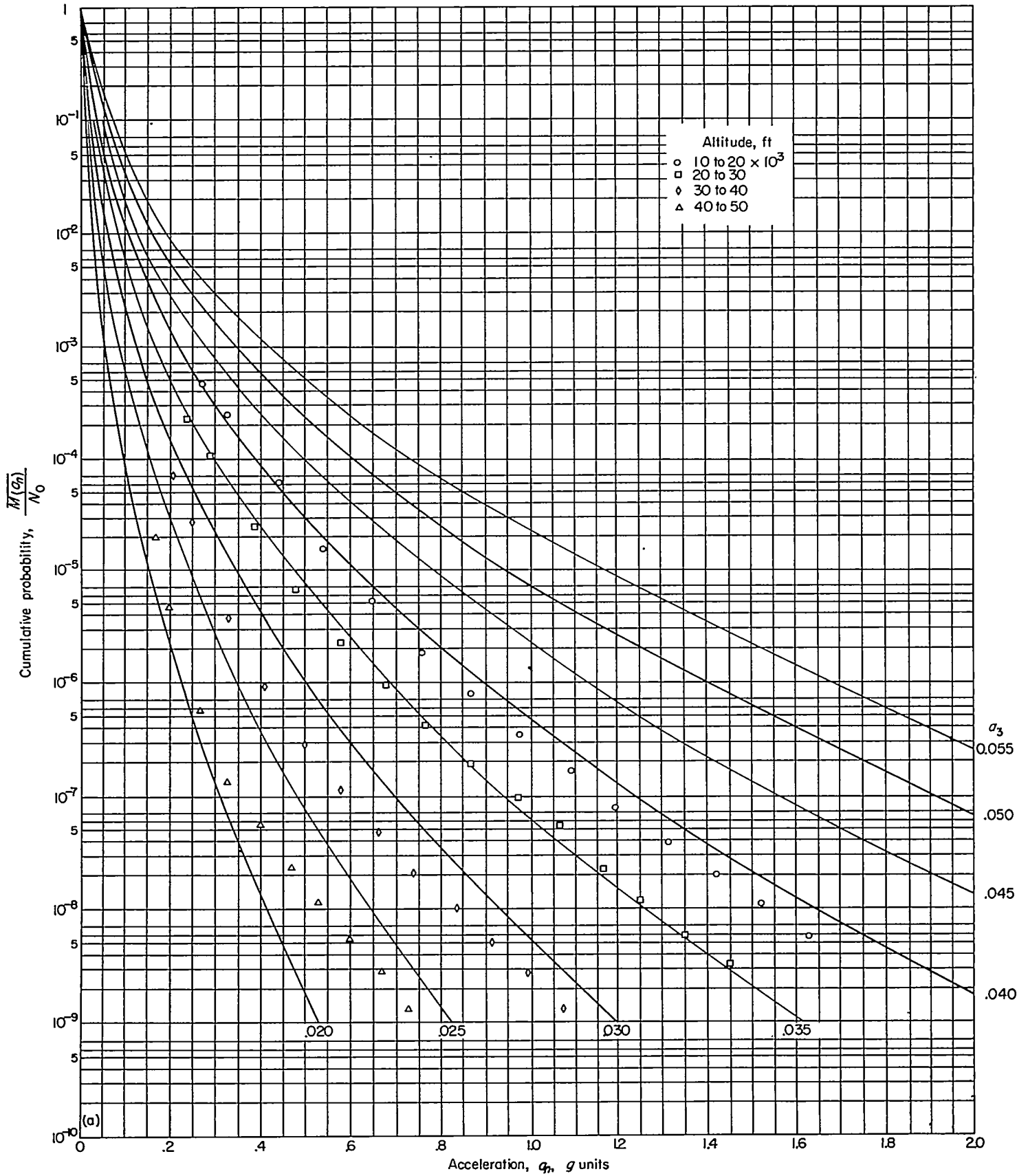
for both altitude brackets of 10,000 to 20,000 feet and 20,000 to 30,000 feet,

$$\hat{f}(\sigma_v) = \frac{1}{2(0.32)^2} e^{-\sqrt{\sigma_v}/0.32} \quad (33)$$

and for both altitude brackets of 30,000 to 40,000 feet and 40,000 to 50,000 feet,

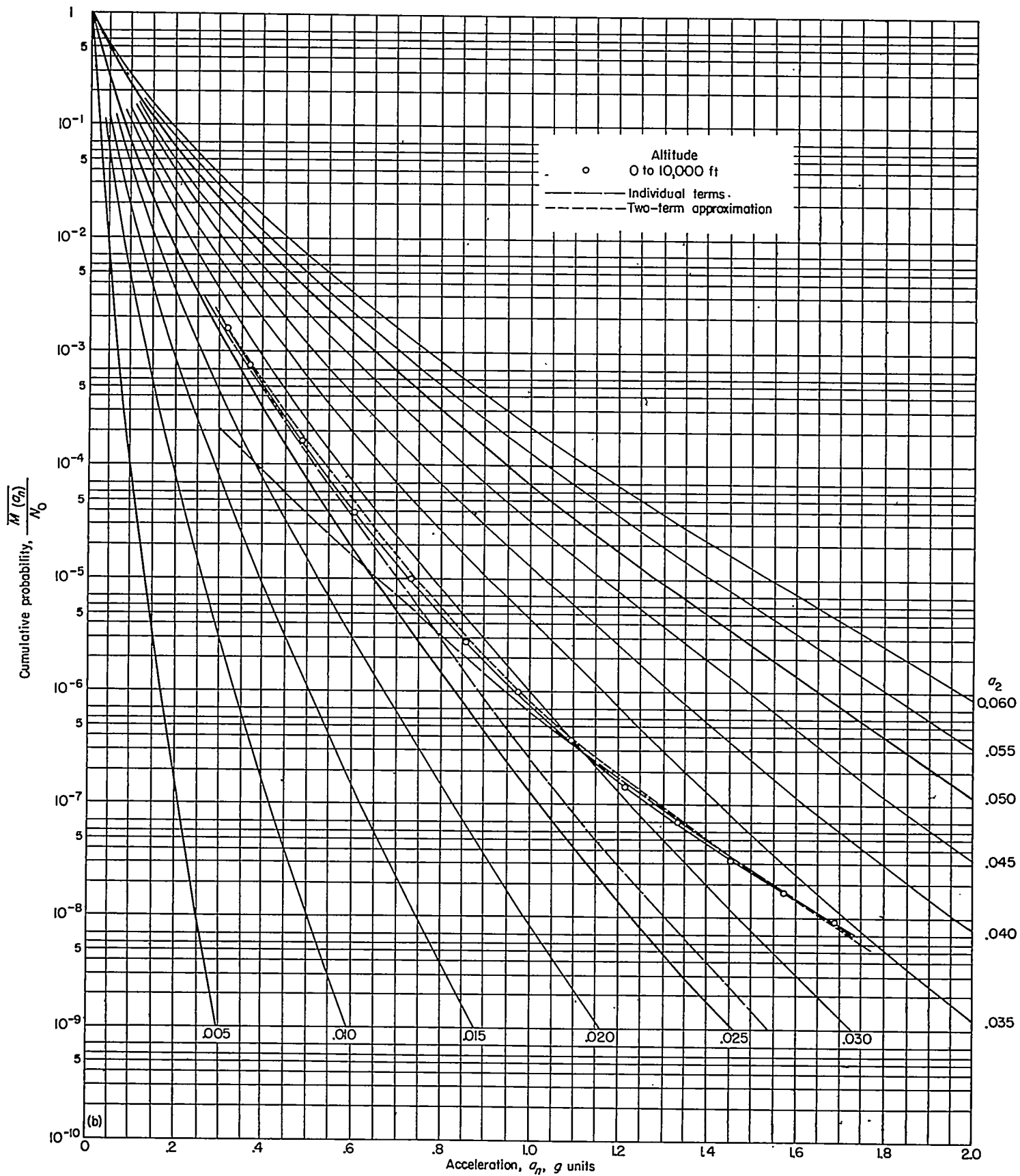
$$\hat{f}(\sigma_v) = \frac{1}{2(0.29)^2} e^{-\sqrt{\sigma_v}/0.29} \quad (34)$$

In both equations (33) and (34) average values of  $b_3$  are given for the two 10,000-foot intervals covered. These distributions are shown in figure 11 (a). The cumulative distributions are shown in figure 11 (b) and give the probability of exceeding given values of  $\sigma_v$ .



(a) 10,000 to 50,000 feet.

FIGURE 10.—Probability of a peak acceleration exceeding a given value of  $a_n$  for a representative transport in flight at various altitude brackets.



(b) 0 to 10,000 feet.

FIGURE 10.—Concluded.

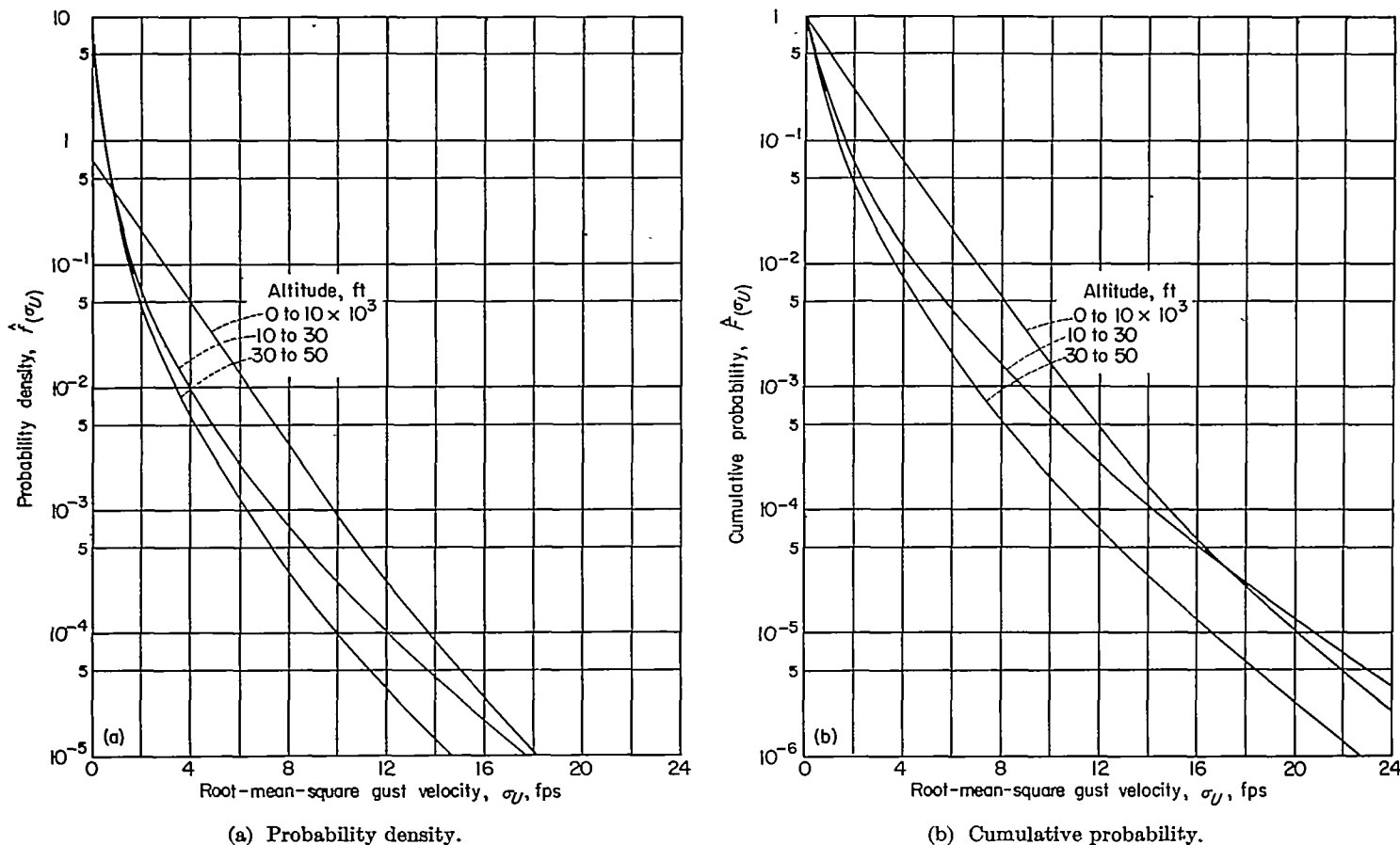


FIGURE 11.—Distribution of  $\sigma_v$  with altitude for routine operations.

Perhaps the most important points to be noted from figure 11 (a) and figure 11 (b) are the relatively large amount of time spent in essentially smooth air at the higher altitudes ( $\sigma_v < 2$  feet per second 93 to 96 percent of the time) and the relatively large amount of time spent in light to severe turbulence at the lowest altitude bracket ( $\sigma_v > 2$  feet per second 25 percent of the time). The time spent above 5 feet per second for the lowest altitude bracket is roughly five to ten times as great as that for the higher altitude brackets.

It should be remembered that these results are in terms of true gust velocity. If equivalent gust velocities which are more directly related to the airplane response are used, the decrease in turbulence intensity with altitude would, of course, be even more pronounced than is indicated herein.

**Method of application.**—The method of application of these results to the calculation of response histories for arbitrary flight is based on the following relation:

$$\overline{M(a_n)} = N_0 \int_0^{\infty} \hat{f}(\sigma_v) e^{-\frac{a_n^2}{2(\bar{A}\sigma_v)^2}} d\sigma_v \quad (35)$$

which is obtained by substituting equations (22a) and (23b) into equation (9). The procedure involves the division of the operational flight plan into homogeneous portions or segments in regard to flight altitude and operating conditions such as airspeed and airplane weight. The appropriate distribution of the root-mean-square gust velocity is

selected for each flight segment from figure 11 (a) and equation (35) is then evaluated for each segment. Actual numerical calculations are facilitated by the use of the charts of figure 6. The sequence of steps involved in such application is as follows:

(1) The operational flight plan is divided into homogeneous segments in regard to flight altitude (10,000-foot altitude brackets) and operating conditions such as airspeed and weight.

(2) The appropriate distribution of  $\hat{f}(\sigma_v)$  is selected for each altitude bracket from figure 11 (a).

(3) The values of  $\bar{A}$  are determined for each significant segment of the flight plan in accordance with equation (22) or (22c).

(4) In order to obtain the associated distributions of acceleration  $f(\sigma_{a_n})$ , each of the distributions of  $\hat{f}(\sigma_v)$  is transformed by the relation

$$f(\sigma_{a_n}) = \frac{1}{\bar{A}} \hat{f}(\sigma_v)$$

where

$$\sigma_v = \sigma_{a_n} / \bar{A}$$

(5) The values of  $N_0$  are most easily determined from flight records, if available, by the methods already indicated. For new designs  $N_0$  must be estimated analytically.

From equations (4) and (20)

$$N_0 = \frac{1}{2\pi} \left[ \frac{\int_0^\infty \omega^2 \Phi_U(\omega) T^2(\omega) d\omega}{\int_0^\infty \Phi_U(\omega) T^2(\omega) d\omega} \right]^{1/2}$$

The reliable estimation of  $N_0$  from this relation is a difficult problem inasmuch as the value depends heavily on the reliability of both the gust spectrum and the airplane frequency response function at the higher frequencies. In order to obtain reliable estimates of this quantity, it appears necessary to account for the effects of spanwise variations in turbulence which act strongly to attenuate the airplane response at these higher frequencies. The effects of the spanwise variations of turbulence on the airplane response have been studied in references 6 and 23 and will have to be considered further in order to establish how best to account for these effects in estimating the value of  $N_0$  by analytical means.

(6) The distributions of  $\sigma_{a_n}$  and the values of  $N_0$  are then used in equation (9) to derive the number of peak accelerations per second or per mile for each condition. These calculations are facilitated by the use of charts such as given in figure (6).

(7) The results obtained in step 6 are then weighted in accordance with the flight distance in each condition or segment and then summed for all conditions in order to obtain the overall acceleration history.

#### VARIATION WITH WEATHER CONDITION

In the preceding discussion, the variation in the gust experience with flight altitude was considered. Another breakdown of the gust experience which may be useful in some problems is the variation in gust experience with weather conditions. Figure 12 (a) shows estimates of the variations in  $\hat{f}(\sigma_U)$  that have been obtained from data for several types of turbulent weather conditions (ref. 24). The curve for clear-air turbulence was based on data obtained in flight through clear and turbulent air at the lower altitudes. The curve for cumulus clouds was based on data obtained in flight under moderate convective conditions such as represented by bulging cumulus clouds. Finally, the curve for thunderstorms was based on data obtained in flight in the immediate vicinity of or within severe thunderstorms. Inasmuch as the data of reference 24 showed a linear variation of the logarithmic gust frequency with gust intensity, the probability distributions of  $\sigma_U$  is given by case a (fig. 6 (a)). The curves of figure 12 (a) are thus given by the equation for case a:

$$\hat{f}(\sigma_U) = \frac{1}{b_1} \sqrt{\frac{2}{\pi}} e^{-\sigma_U^2/2b_1^2} \quad (\sigma_U \geq 0)$$

The values obtained for  $b_1$  are as follows:

For clear-air turbulence,

$$b_1 = 3.15$$

for cumulus clouds,

$$b_1 = 6.28$$

and for thunderstorms,

$$b_1 = 10.05$$

A simple linear measure of the relative intensity of the turbulence for these conditions may be obtained by comparing the values of  $b_1$ . It will be noted that the values of  $b_1$  for the cumulus and thunderstorm conditions are roughly two and three times that for the clear-air condition. The cumulative probability distributions for the three weather conditions are shown in figure 12 (b).

It has been estimated that contemporary transport operations spend about 10 percent of their flight time in this clear-air-turbulence condition, 1 percent in the cumulus condition, and perhaps 0.05 percent in thunderstorms. These results may therefore be applied in evaluating the effects on the overall load experience of operational procedures which would tend to modify this weather experience. For example, the introduction of airborne radar for weather avoidance may be expected to reduce the exposure time to the severe turbulence conditions of thunderstorms. Also, high rates of climb and descent through the lower and more turbulent altitude layers may cause a drastic reduction in the 10 percent of the flight time attributed to clear-air-turbulence conditions and thereby cause a marked reduction in the overall gust experience.

#### RELIABILITY OF RESULTS

The foregoing analysis has indicated that, under reasonable assumptions, available gust statistics in the form of counts of acceleration and gust peaks may be converted into a form suitable for applications in spectral calculations of airplane responses. The appropriate form for this purpose is the probability distribution of the root-mean-square gust velocity. Estimates of this distribution are derived from data for a number of transport operations, and the variation of this distribution with altitude and weather condition is also given. In the derivation of these results, a number of assumptions were made and these assumptions may affect the reliability of the results obtained and their method of application in response calculations. The reliability of the results and the method of applying these results are discussed in this section.

The principal errors in the present analysis stem from the following sources:

- (1) The assumption of the form of the turbulence spectrum and the assumed value of 1,000 feet for the scale of the turbulence
- (2) The assumption of average values of weight, altitude, and airspeeds in the reduction of the data
- (3) The restriction of the airplane dynamics to the one-degree-of-freedom case in the conversion of the results from acceleration to gust velocity
- (4) The assumption that the gusts are uniform across the span
- (5) The statistical sampling errors that arise from the limited data considered.

The magnitude of the errors resulting from each of these sources is considered in turn.

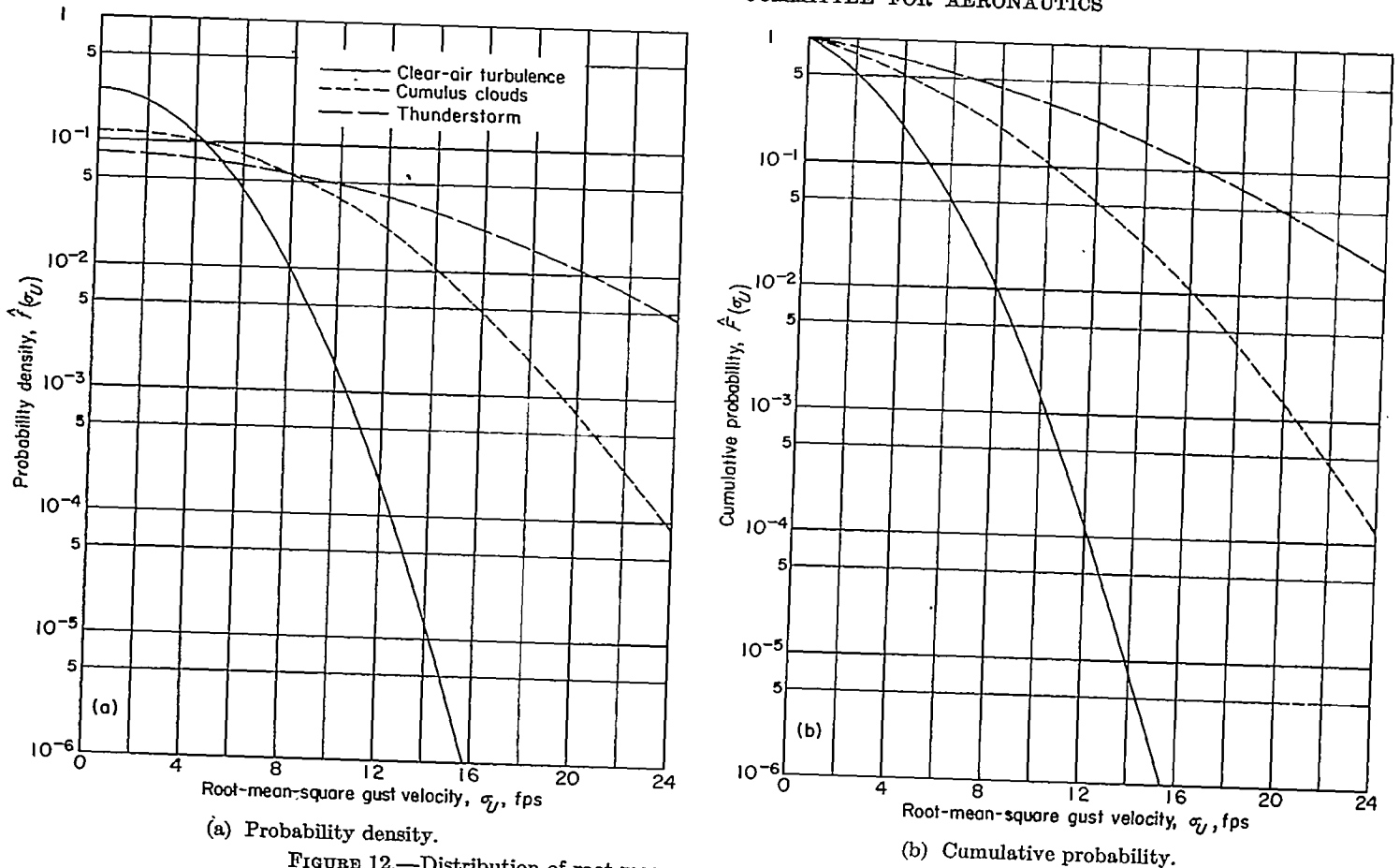


FIGURE 12.—Distribution of root-mean-square gust velocity with weather condition.

**Turbulence spectra.**—The assumed spectral shape given by equation (1) appears to be a reasonable representation of the spectra measurements reviewed in figures 1 and 2 for the region of gust wavelengths covered (10 feet to perhaps 10,000 feet). At the shorter gust wavelengths, the spectrum probably approaches zero at a faster rate than that assumed. However, the contribution of these higher frequencies to the total power is very small and appears negligible.

At the very low frequencies (say, gust wavelengths greater than 3,000 feet), the spectrum is not yet adequately defined although the available measurements suggest a flattening of the spectrum in this region and values of  $L$  of the order of 1,000 feet. It may be expected that the value of  $L$  varies somewhat with weather condition and, as previously indicated, such variations would affect the reliability of the derived root-mean-square gust velocities. This assumption thus appears to be a possible source of error in the distributions of root-mean-square gust velocities derived herein.

The consequences of such possible errors in the scale of turbulence and in the root-mean-square gust velocities on the reliability of load and other response calculations will vary depending upon the airplane response characteristics and have to be evaluated in each case. For many airplanes, the errors in the calculated loads may be largely compensating inasmuch as the errors in the values of root-mean-square gust velocity will be balanced by the error due to the use of the erroneous value of  $L$  ( $L=1,000$  feet) in the calculation of the quantity  $\bar{A}$ . This condition can be verified in a concrete fashion for the one-degree-of-freedom case by some trial calculations by use of the curves for the gust response factor of

figure 7 and consideration of possible variations in the value of the scale of turbulence. For example, representative values of the mass parameter and the mean chord for the airplanes used to collect the gust data are 100 and 10 feet, respectively. For these values and the scale of turbulence of 1,000 feet, the value of  $s = \frac{\bar{c}}{L}$  is 0.01 and the value of the gust response factor  $\sqrt{\frac{I(K,s)}{\pi}}$  is 0.465. If the true value of

the scale of turbulence is 2,000 feet, the value of  $\sqrt{\frac{I(K,s)}{\pi}}$  is about 0.36. The use of the higher value of the gust response factor would, from equation (22), yield a root-mean-square gust velocity that is about 29 percent too low. However, the determination of the value of  $\bar{A}_1$  for the airplane for which the loads are being calculated would, in turn, be high by about the same amount for many cases. For example, for the same mean chord but with a mass parameter of 200, the value obtained for the gust response factor in figure 7 is about 0.61 for  $L=1,000$  feet, as compared with the value of 0.48 for the scale of turbulence of 2,000 feet. Thus, the use of a value of  $L=1,000$  feet in the load calculation yields a compensating error of about 27 percent. Thus, at least for limited variations in the airplane parameters, the net errors in the load calculation due to variation in the scale of turbulence from the assumed value of 1,000 feet would be small.

**Average values of airplane parameters.**—The effects of assuming average conditions of weight, altitude, and speed may also be expected to introduce some errors in the derived root-mean-square gust velocities given in figure 9 for the



various operations. The errors resulting from the assumptions of average weight and altitude may be expected to be small because these errors should largely average out. The effects of speed variations are in a somewhat different category inasmuch as efforts are normally made to reduce speed in rough air. For the operations considered herein (fig. 9), it appears that the reductions in speed from normal operating speeds were generally small and negligible at the lighter levels of turbulence. At the more severe levels of turbulence, the airspeeds were, on the average, somewhat lower than normal operating speeds, but the reductions in most cases were small, about 5 to 10 percent. Thus, the distribution of  $\sigma_V$  at the higher levels may be biased to this extent.

In deriving the results on the variation of the distributions of root-mean-square gust velocity with altitude and weather condition, figures (11) and (12), the assumption of an average speed was not necessary inasmuch as the original distributions of derived gust of reference 8 were largely based on data in which the actual speeds were taken into account. However, average conditions of altitude and weight were assumed both in the derivation of the basic data and in the present reductions. The errors due to these sources should be largely self-balancing and therefore small.

**Airplane dynamics.**—In the derivation of the root-mean-square gust velocities, the airplane was assumed to be rigid and restrained in pitch although free to move vertically. These assumptions are admittedly rough approximations and their effects on the derived gust data require additional study. Extensions of the present results to include the effects of these two additional degrees of freedom appear possible although they would involve a considerably larger number of airplane and operating parameters. It should, however, be possible in the meantime to make some rough overall corrections to the root-mean-square gust velocities for some of these effects. For example, available information suggests that the neglect of the dynamic structural-response effects on the center-of-gravity accelerations might be expected to have resulted in roughly a 10-percent overestimation of the root-mean-square gust velocities for most of the airplanes considered in the present study. The effects of the airplane pitching motions on the root-mean-square gust velocities for the present airplanes are also generally considered small. Recent studies suggest that the pitching motions for the present airplanes would tend to decrease the gust accelerations and thus tend to lead to some underestimation of the root-mean-square gust velocities. A rough estimate of about 10 percent appears reasonable for this effect for the airplanes considered. Thus, it is suggested that the overall effects of pitch and flexibility might largely cancel each other. However, additional study of these effects is needed.

**Effect of spanwise variations in turbulence.**—In the present analysis, no consideration has been given to the effects of gust averaging introduced by the finite span. If the ratio of the span to the scale of turbulence is large, these effects, as has been indicated in reference 6, may be appreciable. For example, for a span of 150 feet and a value of  $L=1,000$  feet, the results of reference 6 suggest that the root-mean-square value of  $\sigma_V$  may be underestimated in the present analysis by perhaps as much as 5 to 10 percent. For smaller values of the ratio of the span to the scale of

turbulence, the magnitude of this discrepancy is considerably smaller. If desirable, the incorporation of these effects on an average basis would also appear straightforward.

**Statistical reliability of results.**—Since the present results are based on relatively small operational samples (of the order of 1,000 hours), the statistical reliability of the desired distributions of root-mean-square value is dependent upon the statistical reliability of the acceleration data. Past experience has indicated that these distributions are reliable for samples of this size at the lower levels of acceleration (0.3g to 0.5g) but have poor statistical reliability at the higher acceleration values. As a consequence, it may be expected that the derived probabilities for the higher root-mean-square gust velocities are only rough estimates and should be used only as a guide. More reliable information regarding the higher root-mean-square gust velocities requires more extensive flight data although it may be possible to supplement the present results by use of available NACA V-G records. The extension of the present applications to include such other data is, however, beyond the scope of the present report.

**Applicability of results.**—In view of the foregoing considerations, the distribution of root-mean-square gust velocity given herein may be considered a reasonable first-order estimate of the characteristics of atmospheric turbulence that are essentially independent of the characteristics of the airplanes involved. Thus, these gust spectra and root-mean-square gust-velocity distributions can be reasonably applied in gust-load calculations in which the effects of pitching motions and flexibility are included in the determination of the airplane transfer functions.

A final word of caution is appropriate in regard to the limitations of the present results, particularly figure 11, for response calculations. Inasmuch as the basic data on which the present results are based were largely obtained from conventional American transport-type operations, they are representative of such operations in regard to such factors as geography, turbulence avoidance procedures, and terrain clearance. As a consequence, the present results may require modification for operations that differ in a significant fashion from those considered herein.

#### CONCLUDING REMARKS

The foregoing analysis has served to demonstrate that the gust statistics may, under reasonable assumptions, be converted into a form appropriate for spectral-type calculations. The significant and fundamental quantity, for this purpose, appears to be the probability distribution of the root-mean-square gust velocity. The results obtained in defining the variations of this function with type of operation, flight altitude, and weather condition provide at least a starting basis for their application to response calculations in arbitrary operations. These results should serve to supplement the discrete-gust techniques in current use and be particularly appropriate in problems requiring a more detailed accounting for the airplane dynamics than is possible by discrete-gust techniques.

## APPENDIX

### RELATIONS BETWEEN PEAK COUNTS AND SPECTRA FOR A GAUSSIAN RANDOM PROCESS

In the present analysis, use is made of the relations between the number of maximums per second and the spectra for a Gaussian random process. These relations are derived in reference 13 and are summarized herein in order to permit the examination of the reliability of the approximate expression used in the body of the report.

#### NUMBER OF MAXIMUMS

The probability  $p_m$  that a Gaussian random process  $y(t)$  will have a maximum intensity ranging from  $y_1$  to  $y_1 + dy_1$  in the time interval  $t$  to  $t + dt$  is given in reference 13 as

$$p_m = dy_1 dt \frac{(2\pi)^{3/2}}{M_{33}} \left[ |M|^{1/2} e^{-M_{11}y_1^2/2|M|} + M_{13}y_1 \left( \frac{\pi}{2M_{33}} \right)^{1/2} e^{-y_1^2/2\psi_0} \left( 1 + \operatorname{erf} \frac{M_{13}y_1}{(2|M|M_{33})^{1/2}} \right) \right] \quad (A1)$$

where the error function is

$$\operatorname{erf} Z_1 = \frac{2}{\sqrt{\pi}} \int_0^{Z_1} e^{-z^2} dz$$

and the coefficients  $M_{ij}$  can be expressed in terms of the value at zero of the autocorrelation function  $\psi(\tau)$  and its derivatives as

$$\left. \begin{aligned} M_{11} &= -\psi_0'' \psi_0^{(4)} \\ M_{13} &= (\psi_0'')^2 \\ M_{33} &= -\psi_0 \psi_0'' \\ |M| &= -\psi_0'' [\psi_0 \psi_0^{(4)} - (\psi_0'')^2] \end{aligned} \right\} \quad (A2)$$

where

$$\psi(\tau) = \lim_{T \rightarrow \infty} \frac{1}{2T} \int_{-T}^T y(t)y(t+\tau) dt$$

and  $\psi_0''$  and  $\psi_0^{(4)}$  are, respectively, the values at 0 of the second and fourth derivative of the autocorrelation function  $\psi(\tau)$ . The values at zero of the autocorrelation function and its derivatives are in turn related to the power-spectral-density function  $\Phi(\omega)$  by the following relations:

$$\left. \begin{aligned} \psi_0 &= \int_0^\infty \Phi(\omega) d\omega \\ -\psi_0'' &= \int_0^\infty \omega^2 \Phi(\omega) d\omega \\ \psi_0^{(4)} &= \int_0^\infty \omega^4 \Phi(\omega) d\omega \end{aligned} \right\} \quad (A3)$$

Equation (A1) is rather unwieldy, but two simple results of interest may be obtained from it. The first result—the expected number of maximums per second  $N_p$ —is obtained

by integrating over  $y_1$  from  $-\infty$  to  $\infty$  and over  $t$  for a time of 1 second to obtain

$$N_p = \frac{1}{2\pi} (\psi_0^{(4)}/-\psi_0'')^{1/2} = \frac{1}{2\pi} \left[ \frac{\int_0^\infty \omega^4 \Phi(\omega) d\omega}{\int_0^\infty \omega^2 \Phi(\omega) d\omega} \right]^{1/2} \quad (A4)$$

The second result is an asymptotic expression for large  $y_1$  for the number of maximums per second  $N(y_1)$  exceeding given values of  $y_1$ , which can be obtained by integrating an asymptotic approximation to  $p_m$  from  $y_1$  to  $\infty$ ; the result, given in reference 13, is

$$N(y_1) = \frac{1}{2\pi} (-\psi_0''/\psi_0)^{1/2} e^{-y_1^2/2\psi_0} = \frac{1}{2\pi} \left[ \frac{\int_0^\infty \omega^2 \Phi(\omega) d\omega}{\int_0^\infty \Phi(\omega) d\omega} \right]^{1/2} e^{-y_1^2/2\psi_0} \quad (A5)$$

It is of interest to note that the right-hand side of equation (A5) is also the exact expression for the number of crossings per second with positive slope of given values of  $y_1$ .

Equation (A5) is the basic relation used in the present analysis for the number of peaks per second exceeding given values of  $y_1$ . Since it is an approximation for this purpose, the magnitude of the errors introduced in the present analysis by its use is of interest and is considered in the remainder of the appendix.

#### RELIABILITY OF THE APPROXIMATION

Past experience has indicated that in gust-load applications, the approximation given by equation (A5) is in most cases good for values of  $y_1/\sigma > 2$ . For values of  $y_1/\sigma < 2$ , equation (A5) tends to underestimate the number of peak loads to some extent. The magnitude of these errors does not, however, appear to be large and, as will be indicated, has only a very small effect on the reliability of the present analysis.

The magnitude of the error introduced by the approximation for small values of  $y_1/\sigma$  may be indicated by considering the ratio  $N(0)$  to the total number of peaks  $N_p$ . From equations (A4) and (A5), this ratio is given by

$$\frac{N(0)}{N_p} = \frac{\int_0^\infty \omega^2 \Phi(\omega) d\omega}{\left( \int_0^\infty \omega^4 \Phi(\omega) d\omega \right)^{1/2} \left( \int_0^\infty \Phi(\omega) d\omega \right)^{1/2}} \quad (A6)$$

For a low-pass filter, which appears to describe roughly the response of a relatively rigid airplane to turbulence, equation (A6) reduces to

$$\frac{N(0)}{N_p} = \frac{\sqrt{5}}{3} \approx 0.75 \quad (A7)$$

The quantity  $N_p$ , which gives all the maximums, includes some maximums at negative values of  $y_1$ . For the low-pass-filter case, the results of reference 13 indicate that about 15 percent of all maximums are at negative values of  $y_1$ . Thus, the approximation of equation (A5) appears to be roughly 10 percent low for the low-pass-filter case at  $y_1/\sigma=0$ . For increasing values of  $y_1/\sigma$ , this error decreases rapidly and is less than 3 percent at  $y_1/\sigma=0.5$ .

For moderately flexible airplanes of the type considered in the present study, the degree of underestimation of the asymptotic formula is somewhat larger than for the band-pass case. In this case, calculations indicate that equation (A5) appears to underestimate the number of peaks by about 30 percent at  $y_1/\sigma=0$ , 10 to 15 percent at  $y_1/\sigma=1$ , and 2 to 3 percent at  $y_1/\sigma=2$ . The effect of these errors is, however, considerably mitigated in the present applications for the following reason. The total number of peak accelerations exceeding given values is seen from equation (9) to depend in principle upon the whole distribution of root-mean-square values. Actually, for the particular exponential-type functions for  $f(\sigma)$  considered in the present analysis, the principal contributions to  $\overline{M}(a_n)$  arise from values of  $a_n/\sigma_{a_n}$  that range from about 1.0 to 4.0. Thus, the asymptotic expression is being applied principally over the region where the underestimation is only a few percent. Therefore, the errors introduced in the present analysis by the use of the asymptotic formula (eq. (A5)) can be considered negligible.

#### REFERENCES

1. Liepmann, H. W.: On the Application of Statistical Concepts to the Buffeting Problem. *Jour. Aero. Sci.*, vol. 19, no. 12, Dec. 1952, pp. 793-800, 822.
2. Fung, Y. C.: Statistical Aspects of Dynamic Loads. *Jour. Aero. Sci.*, vol. 20, no. 5, May 1953, pp. 317-330.
3. Press, Harry, and Mazelsky, Bernard: A Study of the Application of Power-Spectral Methods of Generalized Harmonic Analysis to Gust Loads on Airplanes. NACA Rep. 1172, 1954. (Supersedes NACA TN 2853.)
4. Clementson, Gerhardt C.: An Investigation of the Power Spectral Density of Atmospheric Turbulence. Ph. D. Thesis, M.I.T., 1950.
5. Press, Harry, and Houbolt, John C.: Some Applications of Generalized Harmonic Analysis to Gust Loads on Airplanes. *Jour. Aero. Sci.*, vol. 22, no. 1, Jan. 1955, pp. 17-26.
6. Diederich, Franklin W.: The Dynamic Response of a Large Airplane to Continuous Random Atmospheric Disturbances. Preprint No. 548, S.M.F. Fund Paper, Inst. Aero. Sci., Jan. 1955.

7. Chilton, Robert G.: Some Measurements of Atmospheric Turbulence Obtained From Flow-Direction Vanes Mounted on an Airplane. NACA TN 3313, 1954.
8. Press, Harry, and McDougal, Robert L.: The Gust and Gust-Load Experience of a Twin-Engine Low-Altitude Transport Airplane in Operation on a Northern Transcontinental Route. NACA TN 2663, 1952.
9. Pratt, Kermit G., and Walker, Walter G.: A Revised Gust-Load Formula and a Re-Evaluation of V-G Data Taken on Civil Transport Airplanes From 1933 to 1950. NACA Rep. 1206, 1954. (Supersedes NACA TN's 2964 by Kermit G. Pratt and 3041 by Walter G. Walker.)
10. Binckley, E. T., and Funk, Jack: A Flight Investigation of the Effects of Compressibility on Applied Gust Loads. NACA TN 1937, 1949.
11. Coleman, Thomas L., Copp, Martin R., Walker, Walter G., and Engel, Jerome N.: An Analysis of Accelerations, Airspeeds, and Gust Velocities From Three Commercial Operations of One Type of Medium-Altitude Transport Airplane. NACA TN 3365, 1955.
12. Coleman, Thomas L., and Walker, Walter G.: Analysis of Accelerations, Gust Velocities, and Airspeeds From Operations of a Twin-Engine Transport Airplane on a Transcontinental Route From 1950 to 1952. NACA TN 3371, 1955.
13. Rice, S. O.: Mathematical Analysis of Random Noise. Pts. I and II. *Bell Syst. Tech. Jour.*, vol. XXIII, no. 3, July 1944, pp. 282-332; Pts. III and IV, vol. XXIV, no. 1, Jan. 1945, pp. 46-156.
14. Connor, Roger J., Hawk, John, and Levy, Charles: Dynamic Analyses for the C-47 Airplane Gust Load Alleviation System. Rep. No. SM-14456, Douglas Aircraft Co., Inc., July 29, 1952.
15. Summers, Robert A.: A Statistical Description of Large-Scale Atmospheric Turbulence. Sc. D. Thesis, M.I.T., 1954. (Also Rep. T-55, Instrumentation Lab., M.I.T., May 17, 1954.)
16. Lappi, U. O.: A Direct Method of Utilizing Flight Data To Determine Space and Spectrum Gust Velocity Distributions and Airplane Gust Performance Function (Low Level Turbulence Study). Rep. No. GM-776-T-45 (Contract AF 18(600)-1550), Cornell Aero. Lab., Inc., Aug. 1955.
17. Notess, Charles B., and Eakin, Grady J.: Flight Test Investigation of Turbulence Spectra at Low Altitude Using a Direct Method for Measuring Gust Velocities. Rep. No. VC-839-F-1 (Contract AF 33(616)174), Cornell Aero. Lab., Inc., July 1, 1954.
18. Crane, Harold L., and Chilton, Robert G.: Measurements of Atmospheric Turbulence Over a Wide Range of Wave Lengths for One Meteorological Condition. NACA TN 3702, 1956.
19. Panofsky, H. A.: Statistical Properties of the Vertical Flux and Kinetic Energy at 100 Meters. Scientific Rep. No. 2 (Contract No. AF19(604)-166), Div. of Meteorology, Pennsylvania State College, July 1, 1953.
20. Lawson, James L., and Uhlenbeck, George E., eds.: *Threshold Signals*. McGraw-Hill Book Co., Inc., 1950, ch. 3.
21. James, Hubert M., Nichols, Nathaniel B., and Phillips, Ralph S.: *Theory of Servomechanisms*. McGraw-Hill Book Co., Inc., 1947, ch. 6.
22. McDougal, Robert L., Coleman, Thomas L., and Smith, Philip L.: The Variation of Atmospheric Turbulence With Altitude and Its Effect on Airplane Gust Loads. NACA RM L53G15a, 1953.
23. Liepmann, H. W.: Extension of the Statistical Approach to Buffeting and Gust Response of Wings of Finite Span. Rep. No. SM-15172, Douglas Aircraft Co., Inc., Feb. 1954.
24. Press, Harry: An Approach to the Prediction of the Frequency Distribution of Gust Loads on Airplanes in Normal Operations. NACA TN 2660, 1952.

TABLE I.—SCOPE OF OPERATIONS

Operation	Route	Flight hours	Flight miles
1	Northern transcontinental.....	834	188,000
2	Rocky Mountains—North and South.....	331	55,500
3	Southern transcontinental.....	678	130,000
4	90 percent east of Mississippi River.....	771	202,000
5	New York to Europe—New York to South America.....	1,079	234,000
6	San Francisco to Honolulu.....	1,953	488,000
7	Northern transcontinental.....	876	235,500
8	Southern transcontinental.....	706	193,500

TABLE II.—AIRPLANE AND OPERATIONAL CHARACTERISTICS

Operation	Gross weight, $W$ , lb	Average weight, $\bar{W}$ , lb	Wing area, $S$ , sq ft	Average chord, $\bar{c}$ , ft	Average flight altitude, ft	Average air density, $\rho$ , slugs/cu ft	Airspeed, $V$ , ft/sec	$m$ , per radian	Mass parameter, $K$	$L=1,000; \sqrt{\frac{l(K, \delta)}{\pi}}$
1.....	39,900	33,915	884	10.1	5,000	0.002049	327	5.0	75.00	0.411
2.....	25,200	21,420	987	10.4	8,000	.001869	246	4.92	44.14	.318
3.....	40,500	34,425	817	9.7	5,000	.002049	281	5.03	83.88	.426
4.....	107,000	90,950	1,650	14.7	10,000	.001758	384	4.93	84.55	.386
5.....	142,500	121,125	1,720	12.9	12,500	.001622	386	5.12	133.08	.597
6.....	142,500	121,125	1,720	12.9	12,500	.001622	366	5.12	133.08	.597
7.....	142,500	121,125	1,720	12.9	12,500	.001622	394	5.12	133.08	.597
8.....	89,900	76,415	1,463	13.7	12,100	.001653	402	4.95	91.20	.495

TABLE III.—NUMBER OF ACCELERATION PEAKS EXCEEDING GIVEN VALUES

$a_n$	Cumulative frequency for various operations <sup>1</sup>							
	1	2	3	4	5	6	7	8
0.3.....	20,609	19,483	5,563	1,888	659	612	909	1,287
0.4.....	-----	4,632	1,350	427	152	132	178	232
0.5.....	1,203	1,288	365	118	40	31	40	60
0.6.....	377	370	104	44	13	10	14	18
0.7.....	124	100	31	17	5	4	5	6
0.8.....	47	35	16	6	2	2	-----	1
0.9.....	26	9	5	2	1	1	-----	-----
1.0.....	7	3	2	-----	1	-----	-----	-----
1.1.....	4	-----	2	-----	1	-----	-----	-----
1.2.....	2	-----	-----	-----	-----	-----	-----	-----
1.3.....	1	-----	-----	-----	-----	-----	-----	-----
Total flight hours.....	834	331.1	678.5	770.8	1,078.5	1,953.4	876.5	706.5

<sup>1</sup>Number includes both positive and negative peaks.

TABLE IV.—RESULTS FOR VARIOUS OPERATIONS

(a) Summary of acceleration experience

	Acceleration experience for operation—							
	1	2	3	4	5	6	7	8
$\sigma_{a_{n1}}$	0.430	0.237	0.323	0.278	0.349	0.364	0.255	0.226
$\sigma_{a_{n2}}$	0.247	0.181	0.181	0.147	0.178	0.171	0.132	0.128
$\sigma_{a_{n3}}$	0.147					0.104		
$\frac{2M_1(2\sigma_1)}{2M_2(2\sigma_2)}$	$4.3 \times 10^{-6}$	$1.35 \times 10^{-4}$	$1.35 \times 10^{-3}$	$1.9 \times 10^{-4}$	$9.5 \times 10^{-7}$	$4.6 \times 10^{-7}$	$9.5 \times 10^{-6}$	$2.85 \times 10^{-3}$
$\frac{2M_2(2\sigma_2)}{2M_3(2\sigma_3)}$	$3.2 \times 10^{-4}$	$6.2 \times 10^{-3}$	$8.8 \times 10^{-4}$	$8.2 \times 10^{-4}$	$6.6 \times 10^{-4}$	$3.7 \times 10^{-3}$	$5.4 \times 10^{-4}$	$1.15 \times 10^{-3}$
$N_0$	1.0	1.0	1.0	0.5	0.5	0.5	0.5	0.5
$2N_2$	0.270	0.270	0.270	0.135	0.135	0.135	0.135	0.135
$P_1$	$1.59 \times 10^{-3}$	$4.99 \times 10^{-4}$	$5.00 \times 10^{-3}$	$1.41 \times 10^{-4}$	$7.04 \times 10^{-6}$	$3.41 \times 10^{-6}$	$7.04 \times 10^{-3}$	$2.11 \times 10^{-4}$
$P_2$	$1.18 \times 10^{-3}$	$2.29 \times 10^{-3}$	$3.15 \times 10^{-3}$	$6.07 \times 10^{-3}$	$4.89 \times 10^{-4}$	$2.74 \times 10^{-4}$	$4.00 \times 10^{-3}$	$8.52 \times 10^{-3}$
$P_3$	$2.74 \times 10^{-3}$					$2.22 \times 10^{-3}$		
$a_2$	0.030	0.034	0.026					0.022
$a_3$				0.041	0.036	0.034	0.037	

(b) Summary of gust experience for  $L=1,000$  ft

	Gust experience for operation—							
	1	2	3	4	5	6	7	8
$\bar{A}_1$	0.01755	0.0166	0.0146	0.0146	0.0129	0.0123	0.0132	0.0156
$\sigma_{v_1}$	24.501	17.289	22.063	18.041	27.033	29.787	19.347	14.515
$\sigma_{v_2}$	14.074	10.904	12.363	10.068	13.788	13.993	10.015	8.221
$\sigma_{v_3}$	8.376					8.511		
$b_2$	1.709	2.048	1.781					1.410
$b_3$				.339	0.317	0.308	0.322	

TABLE V.—AIRPLANE AND OPERATIONAL CHARACTERISTICS USED FOR DISTRIBUTION OF  $\sigma_v$  WITH ALTITUDE

[ $\bar{W}=76,415$  lb;  $S=1,463$  sq ft;  $\bar{c}=13.7$  ft;  $V_i=401.5$  ft/sec;  $m=4.95$  per radian;  $N_0=0.5$  per sec]

Altitude, ft	Air density, $\rho$ , slugs/cu ft	Mass parameter, $K$	$\sqrt{\frac{I(K, s)}{\pi}}$	$\bar{A}_1$	$a_2$	$a_3$	$b_2$	$b_3$
0 to $10 \times 10^3$	0.002049	73.4	0.451	0.01758	0.028 .050		1.479 2.844	
10 to 20	.001496	100.5	.524	.01491		0.040		0.327
20 to 30	.001065	141.2	.583	.01181		.035		.313
30 to 40	.000736	204.5	.669	.00907		.0275		.289
40 to 50	.000468	328.4	.741	.00638		.0225		.282

